2012

Progress Toward the Synthesis of a Potential Inhibitor of Chlamydial Protease-like Activity Factor

Elizabeth M. Regan
Wellesley College, eregan@wellesley.edu

Progress Toward the Synthesis of a Potential Inhibitor of Chlamydial Protease-like Activity Factor

Elizabeth M. Regan

Dr. David R. Haines, Advisor

Department of Chemistry

A Thesis Submitted in Partial Fulfillment of the Requirement for the Bachelor of Arts Degree with Honors in Chemistry at Wellesley College

Spring 2012

TABLE OF CONTENTS

ACKNOWLEDGEMENTS

Professor Haines: Thank you for all of your advice, help and stories over the last three years. Your organic chemistry class is the reason I became a chemistry major and the time I have spent working for you has inspired me to continue studying chemistry in graduate school next year. You taught me how to really think about chemistry, instead of simply memorizing facts. Thank you for believing in me and being a wonderful mentor.

Professor Vardar-Ulu, Professor Arumainayagam, and Professor Stark: Thank you for agreeing to serve on my committee and for being great professors who encouraged and challenged me to become a better student.

The Haines Lab: Thank you for a wonderful time in lab. I had so much fun and wish you all the best of luck!

My family & friends: Thank you for all the love and support throughout the last four years. I would not have survived without you.

ABSTRACT

Chlamydia trachomatis is a bacterial pathogen, which causes the most common sexually transmitted disease in the United States. While reproducing, the bacterium secretes a protease known as Chlamydial Protease-like Activity Factor (CPAF). CPAF blocks immune responses and apoptosis in the host cell. An inhibitor of CPAF could allow an immune response to develop and result in a lasting treatment for Chlamydia. There is one known inhibitor of CPAF, lactacystin. The form of lactacystin that appears to penetrate the cells and inhibit CPAF is omuralide. Omuralide irreversibly inhibits CPAF activity but has also been found to inhibit the host cell proteasome, which is responsible for cell waste disposal. By making modifications to the structure of omuralide it may be possible to synthesize compounds that inhibit CPAF without inhibiting the host cell proteasome. The goal of my research is to synthesize a phenyl analog of omuralide. Synthetic progress toward this analog will be discussed.

INTRODUCTION

Chlamydia Trachomatis

Chlamydia trachomatis is a member of the Chlamydiaceae family, which are intracellular parasites that cause disease in humans. Chlamydia trachomatis was formerly considered a virus, but is now described as a bacteria because it contains DNA, RNA and ribosomes and is able to make its own proteins and nucleic acids. It has an inner and outer membrane but is not able to synthesize its own ATP and therefore is an energy parasite.[1]

Chlamydia trachomatis leads to the most common sexually transmitted disease in the United States, with over four million cases reported annually, and over fifty million cases reported worldwide.[2] Chlamydia trachomatis also leads to an ocular infection, which can cause blindness. There are 500 million people worldwide with this infection and seven million people who are blind because of it.[1] Chlamydia is a dangerous and so called silent disease because it often goes untreated for long periods of time. Twenty five percent of men and thirty percent of women infected with Chlamydia do not show any symptoms. An untreated Chlamydia infection in women can lead to salpingitis or pelvic inflammatory disease and consequently infertility. If a pregnant woman is infected, it can cause serious complications for her baby including an ocular infection and pneumonia.[3]

The most common treatment for Chlamydia is antibiotics, and if treated early these can cure the infection without complications. The most common antibiotics in use today are tetracyclines, azithromycin or erythromycin. There is no developed immunity after successful treatment of the infection, so a person can easily become infected again.[3]

Elementary bodies are the infectious form of Chlamydia trachomatis. They are 0.3 to 0.4 micrometers in size and have a rigid outer membrane. The rigidity is due to cross-linked disulfide bonds. This outer membrane makes the bacteria resistant to the harsh environment outside of eukaryotic cells. The reticulate bodies are the non-infectious, replicated form of Chlamydia trachomatis inside the host cells. Their outer membrane is fragile because of the lack of disulfide bonds.[4]

The developmental cycle of Chlamydia (Figure 1) begins with the binding of the elementary bodies to receptors on eukaryotic cells, most commonly human epithelial cells. The elementary bodies reside in a membrane-bound vacuole, called an inclusion, in the cytoplasm of the host cell, where they replicate into reticulate bodies. In the later stages of development the reticulate bodies become elementary bodies and are released from the host cell to infect neighboring cells.[4] Chlamydia trachomatis injects many effector proteins into the cytoplasm of the host epithelial cell, which allow it to manipulate host cell functions, such as metabolic and signaling pathways. This can lead to modifications in gene expression, redirection of vesicle transport and the blockage of cell apoptosis.[5]

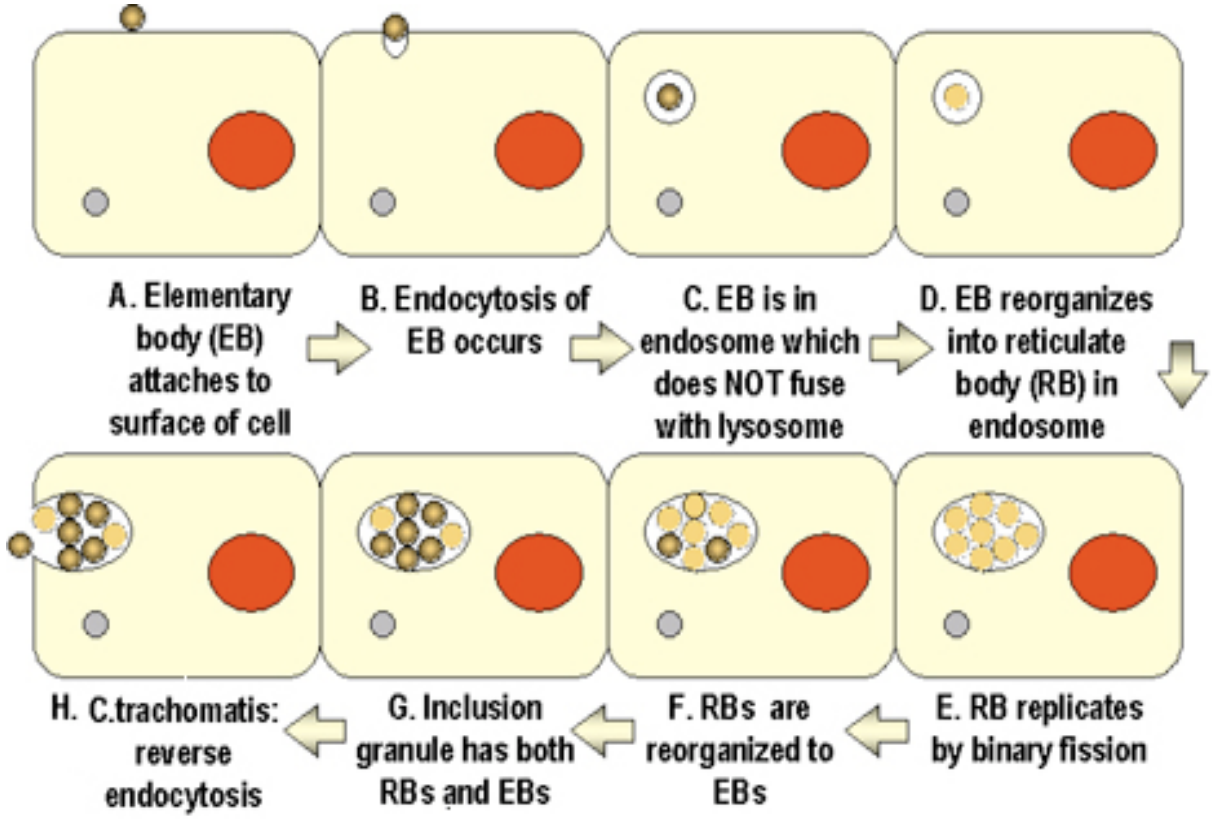

Figure 1: Developmental Cycle of Chlamydia. Figure from Mayer.[1]

Chlamydial Protease-like Activity Factor

Chlamydia trachomatis secretes a protease known as Chlamydial Protease-like Activity Factor (CPAF), which plays a major role in the pathogenesis of Chlamydia (Figure 2). CPAF is secreted into the host cell cytoplasm, where it has a number of roles.[6] The structure of CPAF consists of two subunits, CPAFn and CPAFc.

Separation of CPAFn and CPAFc results in the loss of function of the protease, so it no longer can degrade host cell immune responses.[7]

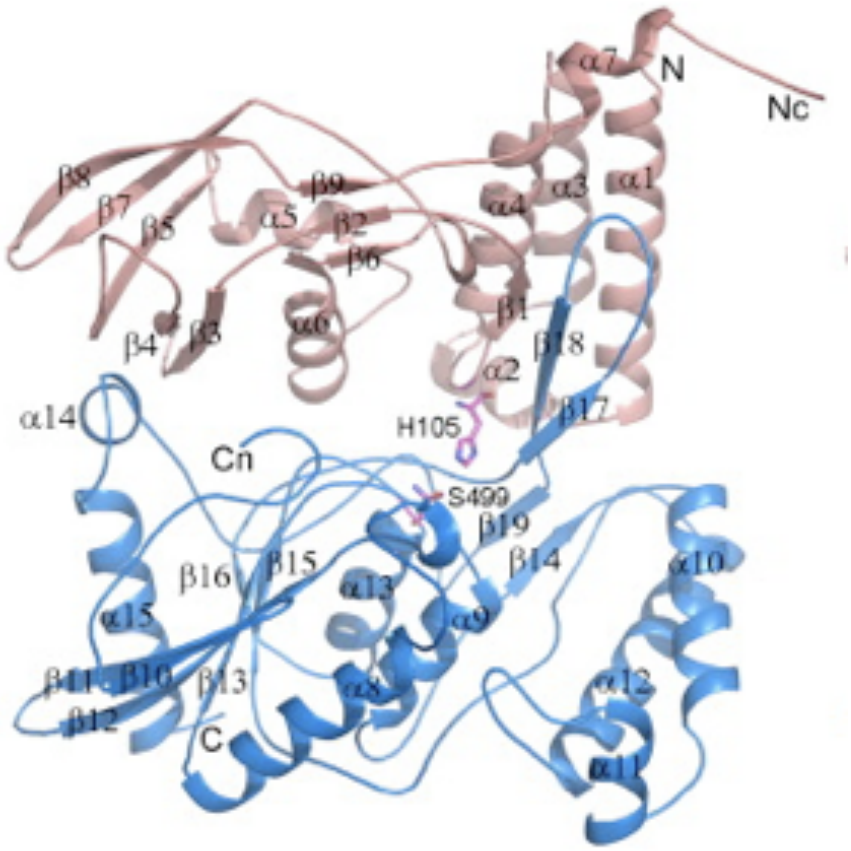

Figure 2: Crystal structure of Chlamydial Protease-like activity factor (CPAF). The two subunits are colored in blue and pink. Figure from Huang *et al.*[6]

CPAF degrades host cell transcription factors, RFX5 and USF-1, inhibiting cell production of antibodies to kill the bacteria.[8] The protease also has the ability to inhibit BH3-only proteins, which can block host cell apoptosis.[8,9] CPAF cleaves the

transcription factor p65/RelA. This transcription factor belongs to the family of transcription factors, NF-*k*B, that are essential to pro-inflammatory signaling. The cleavage of this transcription factor allows the bacteria to prevent the cell's immune response, which would clear the infection by inflammation.[10] A second pro-inflammatory protein, HMGB1, is also cleaved by CPAF.[11]

CPAF cleaves nectin-1, a cell adhesion protein responsible for the formation of cell-cell adhesion between epithelial cells.[12] Cyclin B, which regulates cell mitosis, and PARP, which controls DNA damage during cell apoptosis, are also cleaved by CPAF.[13] Most recently it has been discovered that CPAF activity is necessary for the replication of the bacteria and for preserving the Chlamydia inclusion membrane inside the host cell.[14] The secretion of CPAF by Chlamydia trachomatis is essential for the survival of the bacteria inside the host cell and for the pathogenesis of Chlamydia.

The active site of CPAF sits between the two subunits (Figure 3). CPAF is a serine protease and Ser499 and His105 are necessary for its catalytic activity and therefore are present at the active site. In most serine proteases an Asp residue forms a catalytic triad with the Ser and His residues at the active site. The CPAF active site does not contain an Asp residue, so the catalytic activity is achieved by a different method. A water molecule mediates a hydrogen bond between His105 and Glu558, which activates the Ser499 for catalytic activity. Mutations to either the Ser499 or His105 residues result in a loss of CPAF activity.[6] Knowledge of the active

site of CPAF has lead to anti-chlamydial drug research, especially the development of inhibitors of CPAF activity.

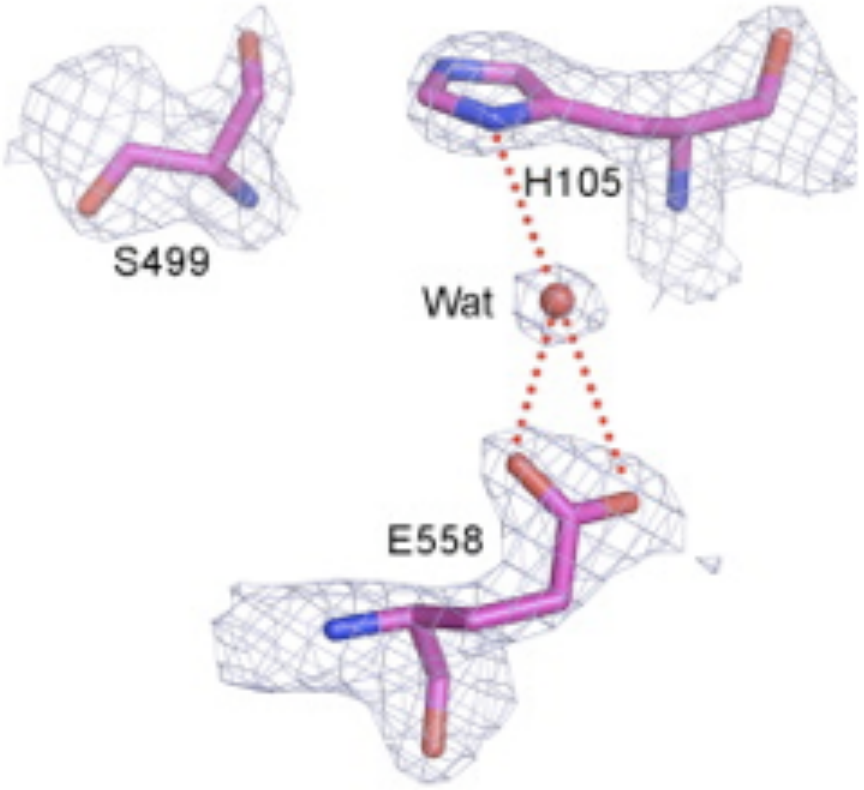

Figure 3: Active site of CPAF. Figure from Huang *et al.*[6]

Omuralide

Omuralide (1) is a known inhibitor of CPAF. Omuralide is the active form of lactacystin (2), a known irreversible proteasome inhibitor (Figure 4). Omuralide covalently binds to the Ser499 residue in the active site of CPAF (Figure 5). Nucleophilic attack by the terminal hydroxyl group on Ser499 on the carbonyl carbon (C6) of omuralide leads to the formation of an ester bond in the CPAF active site.[6] The binding interactions between omuralide and the active site of CPAF lead to irreversible inhibition of CPAF activity. However, omuralide also leads to inhibition of the host cell proteasome, which is essential for cell waste disposal.[15]

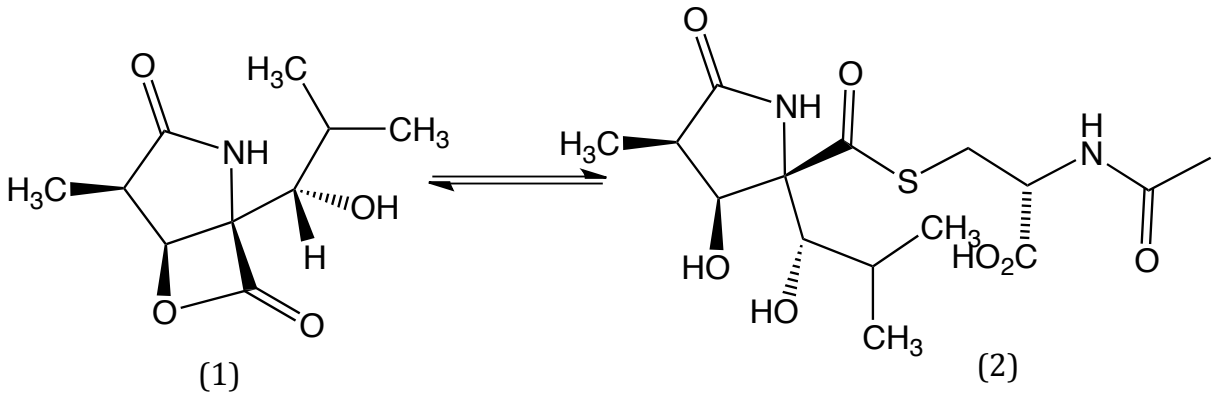

Figure 4: Chemical structures of Omuralide and Lactacystin.[15] The alcohol of lactacystin (2) converts the thio-ester to an ester to give omuralide (1).

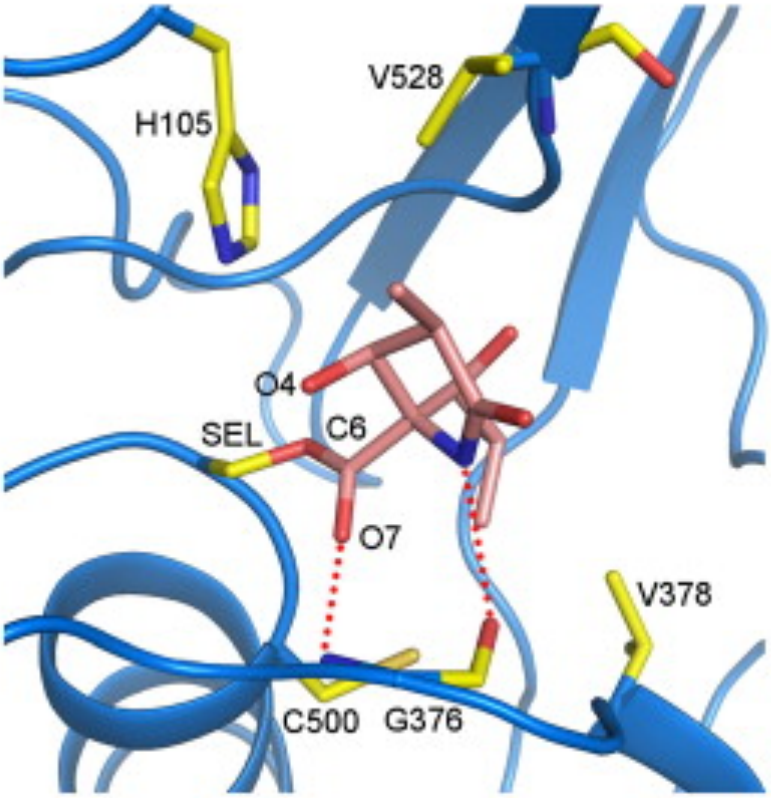

Figure 5: Binding of omuralide to CPAF. Omuralide is shown in pink, the side chains of CPAF are shown in yellow and "SEL" represents the ester product between Ser499 and omuralide. Figure from Huang *et al.*[6]

Development of a CPAF inhibitor that does not affect the host cell proteasome could provide a lasting treatment for Chlamydia. Two substituents on the omuralide molecule have been varied to create structural analogs (Figure 6). By varying either the "R" group or the "X" group many structural analogs of omuralide were synthesized and tested for proteasome inhibition (Table 1). An analog in which the isopropyl group was substituted by a benzene ring did not inhibit the tested proteasome.[15,16,17,18] These analogs were not tested for inhibition of CPAF.

Synthesis of the phenyl-omuralide analog (3) could lead to exclusive inhibition of CPAF and progress toward a new treatment for Chlamydia that generates an immune response.

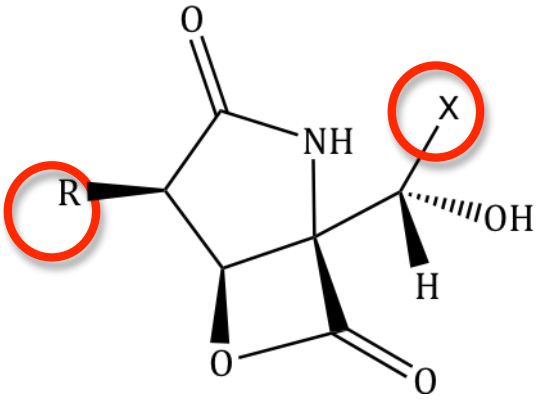

Figure 6: Structure of Omuralide. The two groups, "R" and "X" can be varied on the molecule to produce omuralide analogs that will inhibit CPAF without affecting host cell functions.[15,16,17,18]

Analog Structure	K_{assoc} ($M^{-1}s^{-1}$)	Analog Structure	K_{assoc} ($M^{-1}s^{-1}$)
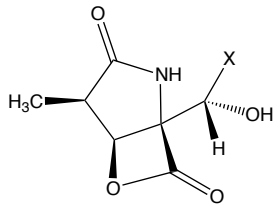		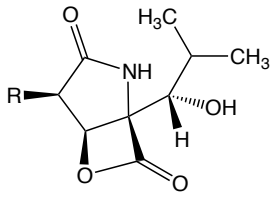	
X= -$CH(CH_3)_2$	3059	R= CH_3-	3059
X= -H	9.7	R= H-	450
X= -C_6H_5	no inhibition	R= CH_3CH_2-	6679
X= -C_2H_5	290	R= $CH_3(CH_2)_3$-	7275
X= -$CH=CH_2$	188	R= $(CH_3)_2CH$-	8465
X= -$CH_2CH_2CH_3$	192	R= $C_6H_5CH_2$-	2227
X= -$CH_2CH=CH_2$	255		
X= -$CH_2CH(CH_3)_2$	17.4		
X= -$CH_2C(CH_3)=CH_2$	64.7		

Table 1: Kinetics of inhibition of β-lactone analogs of omuralide. From Corey *et al.*[18] K_{assoc} describes the strength of binding between two molecules. The larger the K_{assoc} the greater the bonding affinity between the molecule and the proteasome. Strong binding between the analog and proteasome leads to greater inhibition of the cellular proteasome, which is not wanted. Inhibition was measured using the 20 S proteasome from bovine brain, the 20 S proteasome is present in all eukaryotic organisms.

Experimental Goals and Purpose

The goal of my research is the progress toward an efficient synthesis of a phenyl omuralide analog (Figure 7). This compound has been synthesized previously and shown to not inhibit the cellular proteasome, but it is not known whether it inhibits CPAF.[15,16,17,18] This compound is not available from the original source for testing against CPAF. Synthesis of this compound needs careful stereochemical control due to the four chiral centers. The phenyl group must be added as late as possible in the synthesis for the efficient synthesis of other analogs and the β-lactone ring must be closed late. The synthesis being attempted is shorter than the synthesis of the compound done by Corey[15,18] and is based on the synthesis done by Soucy of a potent analogue of clasto-lactacystin β-lactone, for the treatment of ischemia-reperfusion injury.[19] The analog synthesized by Soucy has the isopropyl, like omuralide, instead of the phenyl but instead of the methyl group of omuralide on the ring there is a long alkyl chain.

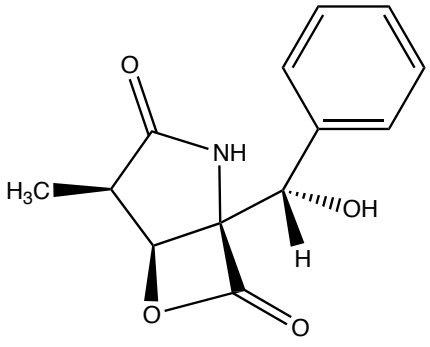

(3)

Figure 7: Structure of the phenyl omuralide analog (3).

The total synthesis of compound 3 (Figure 8) begins with the synthesis of the oxazole (7), a very electron rich species, which can act as a nucleophile. Nucleophilic attack of the carbonyl of benzaldehyde (8) by compound 7 in the presence of an aluminum catalyst gives the oxazoline (9). Deprotonated, compound 9 is then reacted with an amido aldehyde (10) in the presence of the catalyst, dimethylaluminum chloride, to give the aldol product (12). At this point in the synthesis all pieces of the final product are present, the phenyl group and the four chiral centers have been added and the piece of the compound that will become the β-lactone has been installed. From here in a series of six steps protecting groups are removed leaving the final product, compound 3.[20] Once the phenyl omuralide analog has been synthesized it will be sent to our collaborators at Duke University for biological testing to see if it successfully inhibits CPAF.

Like Soucy's synthesis, the major reaction of this synthesis is the aldol coupling of two main intermediates: a chiral aldehyde and an oxazoline.[19] This was the last step successfully completed in this thesis. Characterization of the products of this reaction proved to be difficult and will be discussed further.

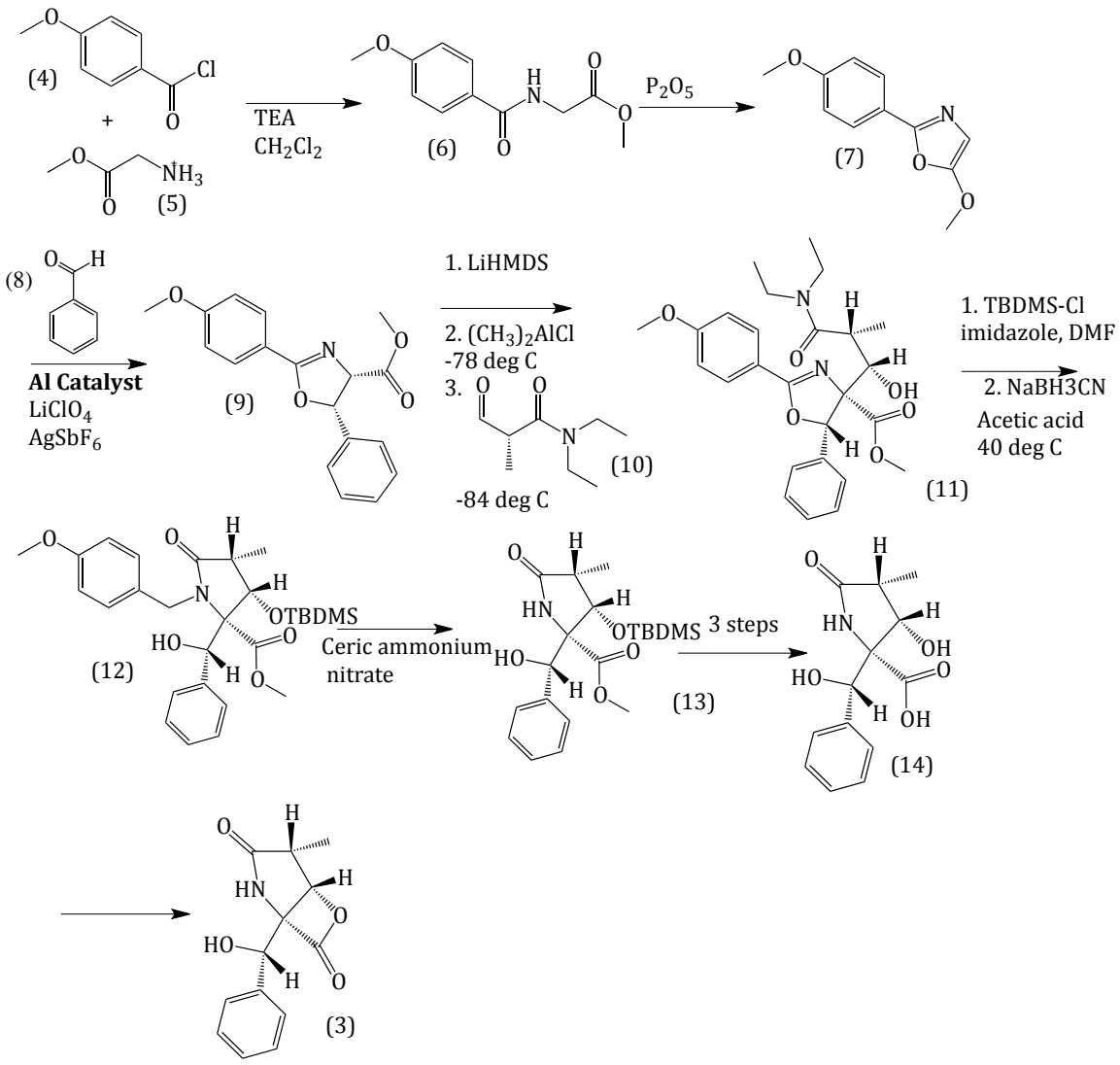

Figure 8: Proposed Synthetic Scheme.[19,20]

RESULTS AND DISCUSSION

I. Synthesis of Amido Aldehyde

In the first step of the synthesis (Figure 9) Methyl (2R)-3-hydroxy-2-methylpropionate (16) was reacted with Benzyl 2,2,2-trichloroacetimidate (17) resulting in nucleophilic substitution (Figure 9). Protonation of the nitrogen on compound 17 by the addition of triflic acid made the oxygen of the imidate a good leaving group and allowed for nucleophilic attack by the alcohol of compound 16 on the electrophilic benzylic carbon of compound 17. The product of this reaction is Methyl (2R)-3-benzyloxy-2-methylpropionate (18).[20,21]

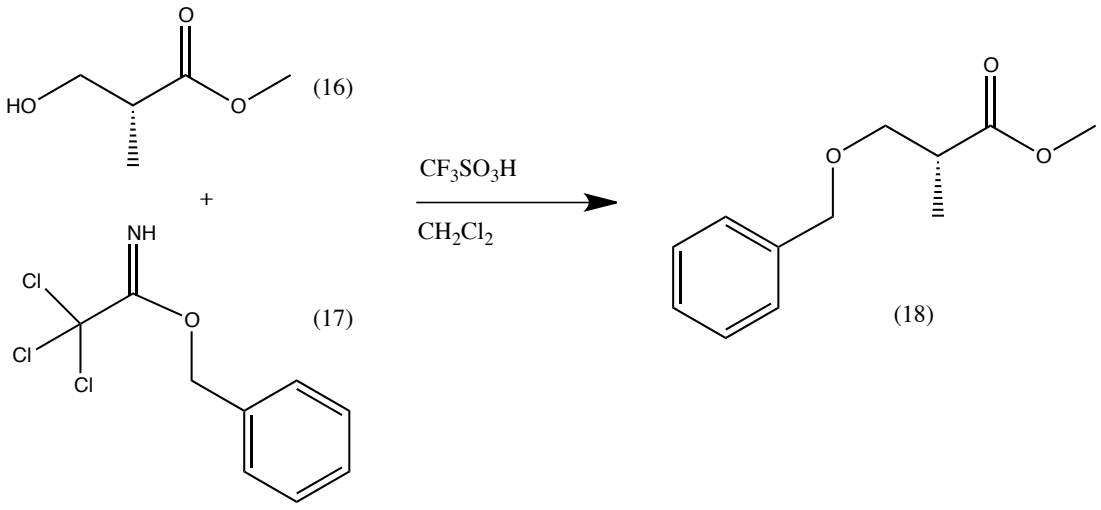

Figure 9: Synthesis of Methyl (2R)-3-hydroxy-2-methylpropionate (18).

Compound 18 was reacted with lithium hydroxide in the presence of water and tetrahydrofuran in a base catalyzed hydrolysis of a carboxylic ester (Figure 10). The oxygen of lithium hydroxide attacks the electrophilic ester carbon breaking the π double bond and creating a tetrahedral intermediate. However, this intermediate is not stable and the double bond between the carbon and oxygen reforms resulting in the loss of methanol as the leaving group and the formation of the carboxylic acid product, (2R)-3-Benzyloxy-2-methylpropionic acid (19).[19,20]

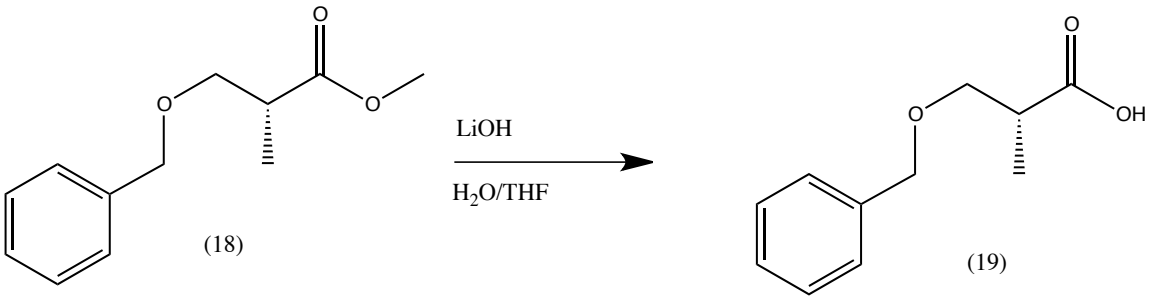

Figure 10: Synthesis of (2R)-3-Benzyloxy-2-methylpropionic acid (19).

Compound 19 was reacted with diethylamine in the presence of the peptide coupling reagent, TBTU, and diisopropylethylamine (Figure 11).[22,23] The diisopropylethylamine deprotonates the carboxylic acid, allowing it to nucleophilically attack the positively charged carbon of TBTU. The hydroxybenzotriazole is a good leaving group, and leaves the rest of the TBTU molecule. The now negative nitrogen of the hydroxybenzotriazole nucleophilically attacks the carbonyl carbon and the remainder of the TBTU leaves. This

hydroxybenzotriazole is a good leaving group, so the nucleophilic nitrogen of the diethylamine was able to attack the electrophilic carbonyl to give 3-Benzyloxy-N,N-diethyl-2-(R)-methylpropionamide (20).[19,20]

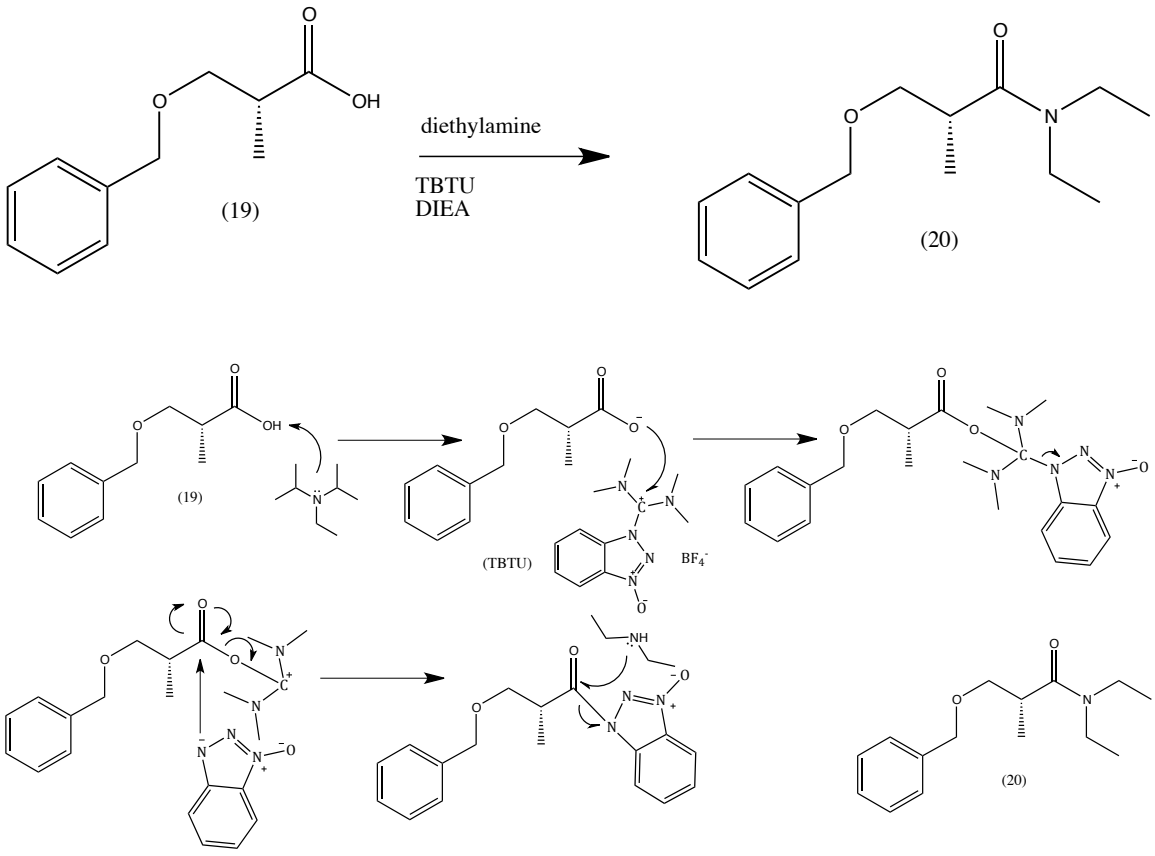

Figure 11: Mechanism of the synthesis of 3-Benzyloxy-N,N-diethyl-2-(R)-methylpropionamide (20).

Compound 20 was reacted with hydrogen gas using the catalyst palladium hydroxide in this catalytic hydrogenation reaction (Figure 12). The benzene of compound 20 was attracted to the surface of the metal and hydrogen atoms were added to the oxygen and the carbon bonded to the benzene breaking the carbon-

oxygen bond and resulting in the product N,N-Diethyl-3-hydroxy-2-(R)-methylpropionamide (21).[19,20,24]

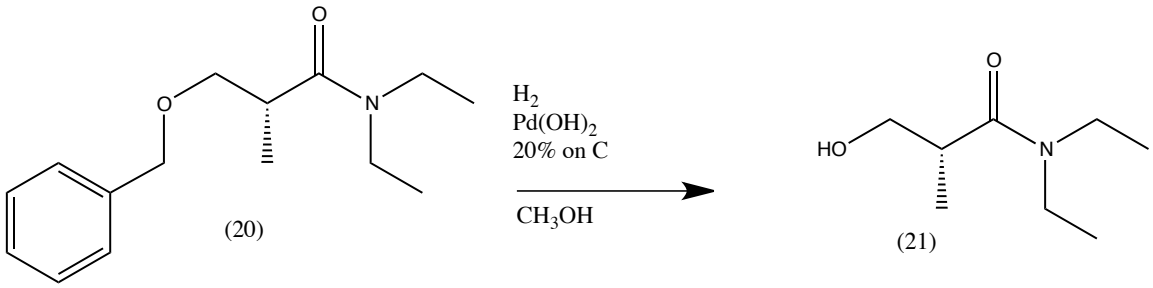

Figure 12: Synthesis of N,N-Diethyl-3-hydroxy-2-(R)-methylpropionamide (21).

In last the step of the synthesis compound 21 was oxidized using the Dess-Martin periodinane reagent (22), which oxidizes primary alcohols to aldehydes under mild conditions (Figure 13).[24] This is important because it prevents over oxidation of the alcohol to the carboxylic acid. First, one of the oxoacetate groups on compound 22 is displaced by the alcohol. Next, a second oxoacetate deprotonates the alcohol carbon. Those electrons fall in to make a double bond between the carbon and oxygen giving the final product, N, N-Diethyl-2-(R)-methyl-3-oxopropionamide (10). This product is not very stable and must be stored at 0° C under nitrogen.[19,20,25,26] It is important to note that compound 10 has a chiral carbon. This will be important later in the synthesis when choosing a catalyst.

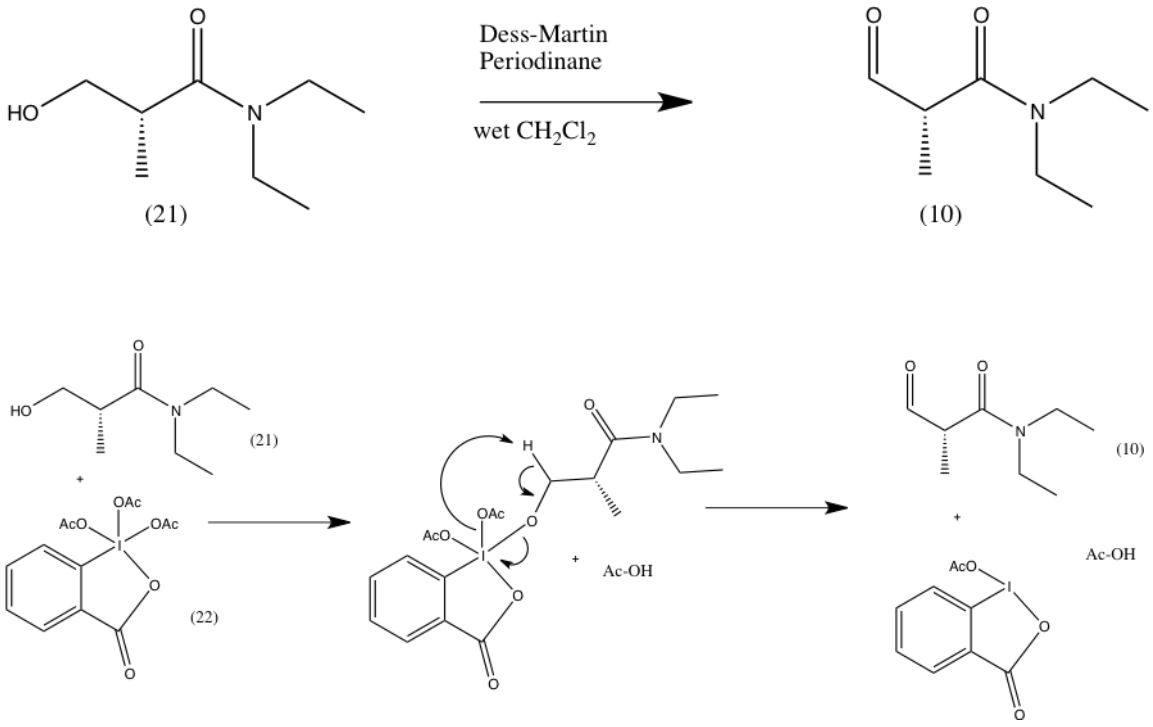

Figure 13: Mechanism of Dess-Martin oxidation.

II. Synthesis of Aluminum Catalyst

In the first step of this two step synthesis, R-(+)-1,1Binaphthyl-2,2'-diamine (23) was reacted with two equivalents of 3,5-di-tert-butyl-2-hydroxybenzaldehyde in an acid catalyzed imine formation (Figure 14). The aldehyde is protonated intramolecularly by the phenol causing the aldehyde carbon to be positively charged. The basic amine substituents on compound 23 then nucleophilically attack the positive carbon. Water leaves and the nitrogen donates its electrons to form the

double bond giving the product (R)-2,2’-bis(3,5-Di-tert-butyl-2-hydroxybenzylideneamino)-1,1’-binaphthyl (24).[20,25,27]

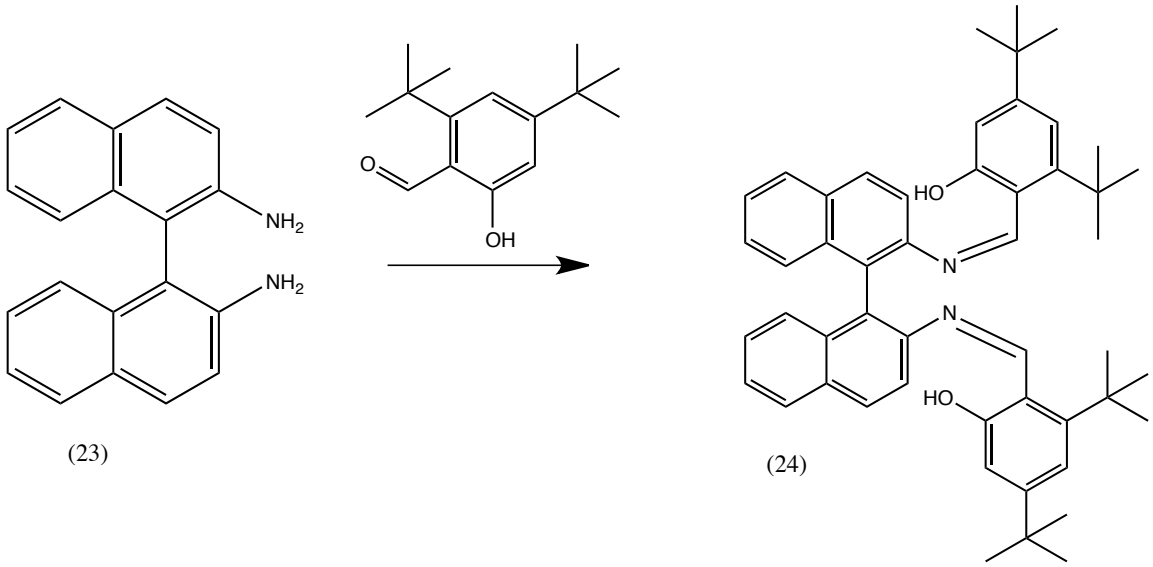

(23) (24)

Figure 14: Synthesis of (R)-2,2’-bis(3,5-Di-tert-butyl-2-hydroxybenzylideneamino)-1,1’-binaphthyl (24).

Compound 24 is then reacted with dimethylaluminum chloride (Figure 15). The methyl groups on the dimethylaluminum chloride are basic and deprotonate the two hydroxyl groups of compound 24. Methane leaves and the aluminum bonds to the oxygens and nitrogens of compound 24 to give (*R*)-2,2'-bis(3,5-Di-*tert*-butyl-2-hydroxybenzylideneamino)-1,1'-binaphthyl aluminum chloride (25).[20,27] Because of the size of this molecule no NMR was taken because it would have been too complicated to interpret. This molecule was used later in the synthesis as a catalyst.

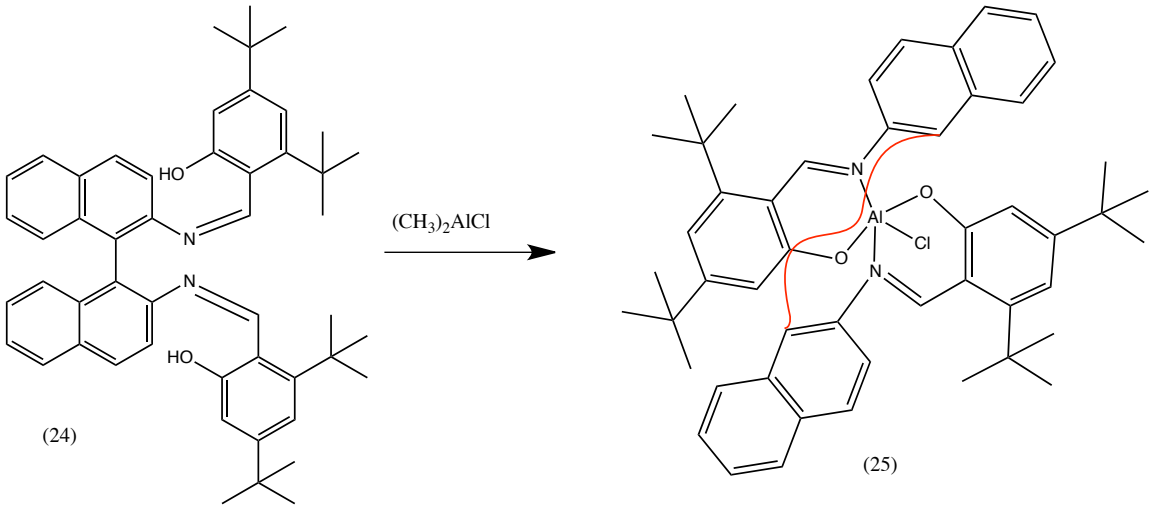

Figure 15: Synthesis of (*R*)-2,2'-bis(3,5-Di-*tert*-butyl-2-hydroxybenzylideneamino)-1,1'-binaphthyl aluminum chloride (25). The red line is a bond between the two carbons.

III. Synthesis of Oxazoline

In the first step of the synthesis of the oxazoline, glycine methyl ester hydrochloride (5) was reacted with methoxybenzoyl chloride (4) in the presence of triethyl amine (Figure 16). Triethyl amine is a base, which is commonly used with acyl chlorides. It acts by removing hydrogen chloride from the mixture, allowing for the formation of the protected activated glycine, N-4-Methoxybenzoylglycine methyl ester (6).[20,28]

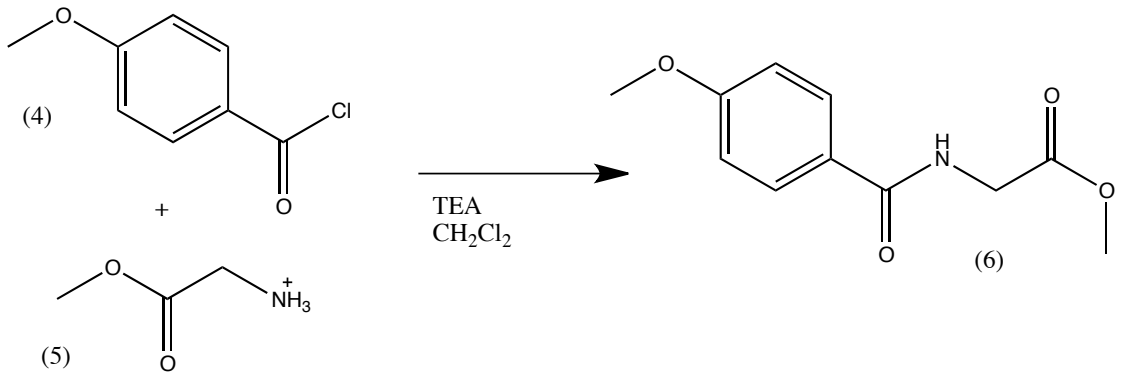

Figure 16: Synthesis of N-4-Methoxybenzoylglycine methyl ester (6).

Next compound 6 was reacted with phosphorous pentoxide, a dehydrating agent (Figure 17). The oxygen of the amide carbonyl is the most negative in compound 6. This oxygen attacks the phosphorous breaking the double bond to the carbon. The nitrogen then donates its electrons in to make a new double bond to the carbon, leaving the nitrogen positively charged. The carbon bound to the nitrogen is now susceptible to intramolecular nucleophilic attack by the ester carbonyl breaking both double bonds and leaving the carbon positively charged. The double bond between the two carbons and the double bond between the carbon and nitrogen are reformed. The oxygen bonded to the phosphorous leaves giving 5-Methoxy-2-p-methoxyphenyloxazole (7).[20,29]

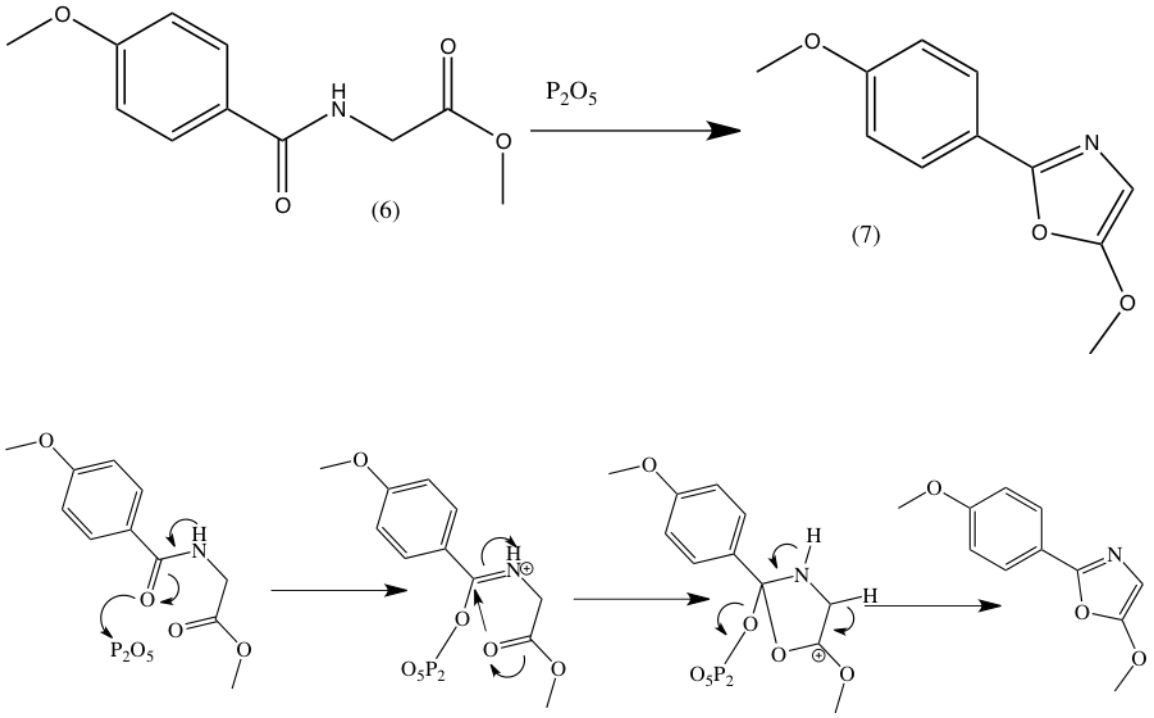

Figure 17: Mechanism of the synthesis of 5-Methoxy-2-p-methoxyphenyloxazole (7).

Compound 7, the oxazole, is an extremely important intermediate in the synthesis. It is highly electron rich as can be seen in Figure 18. This allows the oxazole to act as a nucleophile performing attack from carbon 5 of the oxazole ring, which is partially negatively charged (circled in red).

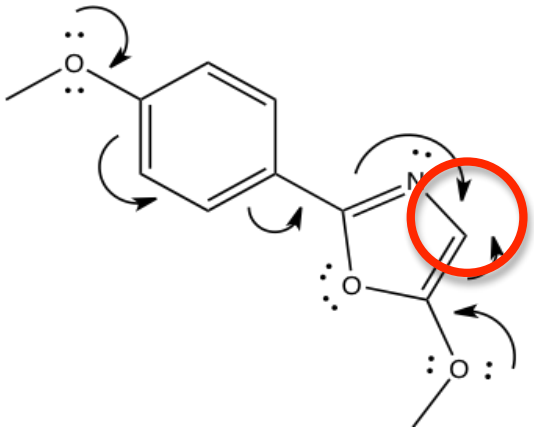

Figure 18: Reactivity of Oxazole (7). Compound 7 can act as a nucleophile at carbon 5 of the oxazole ring, which is circled in red.

In the final step of the synthesis compound 7 is reacted with benzaldehyde (8) in the presence of the previously synthesized aluminum catalyst (25) (Figure 19). The nucleophilic carbon on compound 7 attacks the partially positive carbon on the benzaldehyde. The double bonds are broken to give the oxygen a negative charge and the carbon a positive charge. The negative oxygen then attacks the oxazole carbon between the nitrogen and oxygen, which breaks the double bond to the nitrogen, leaving the nitrogen negatively charged. The nitrogen then donates its electrons to recreate the double bond to the carbon and the oxygen donates its electron to form a double bond with the carbon that was positively charged giving the product, (4R,5S)-2-p-methoxyphenyl-5-phenyl-4,5-dihydrooxazole-4-carboxylic acid methyl ester (9). This mechanism is interesting because the original oxazole ring is broken and a new oxazoline ring is formed, which may not be the expected mechanism from first glance at the starting material and final product.[19,20,27]

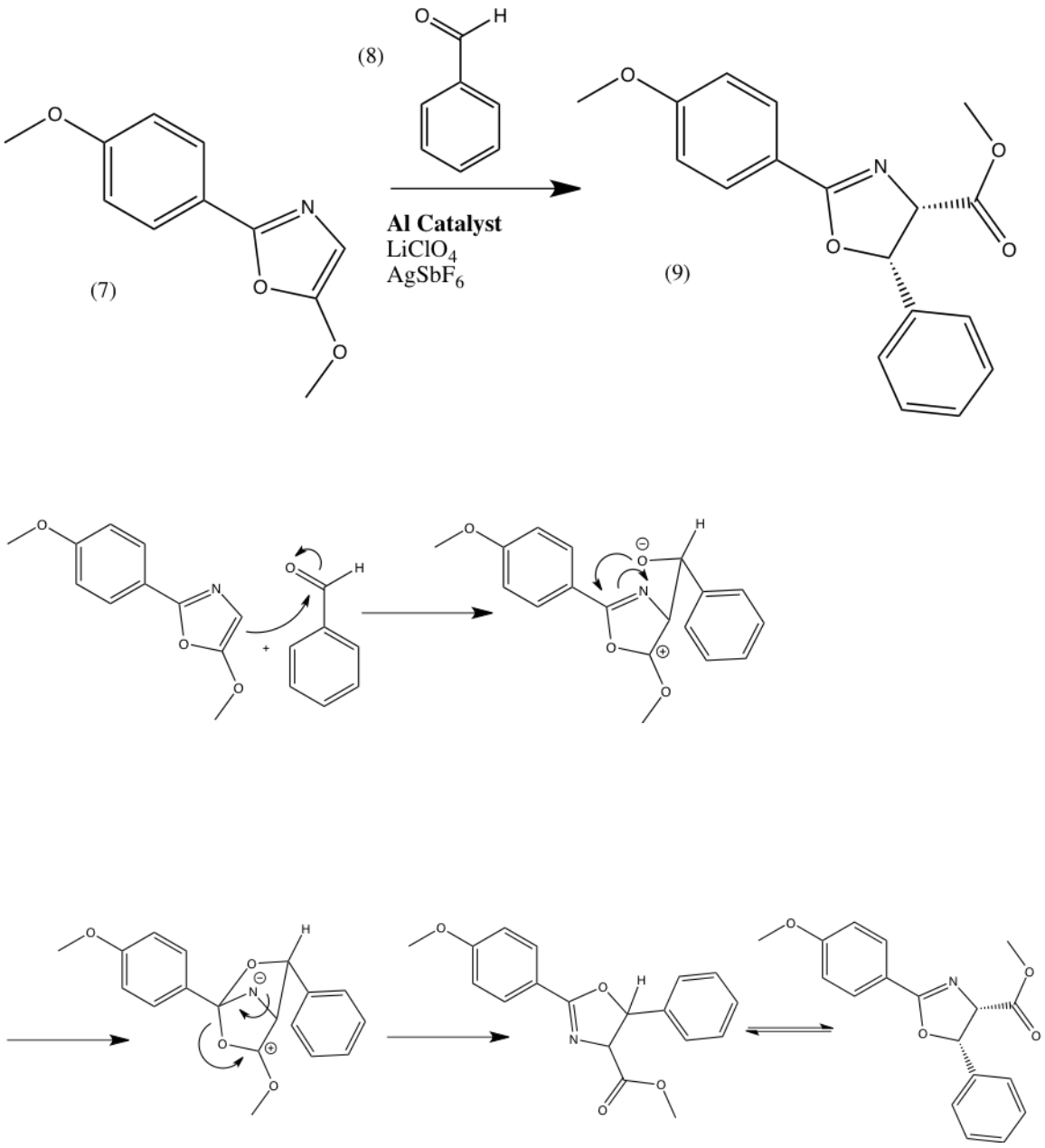

Figure 19: Mechanism of the synthesis of the oxazoline (9).

This synthesis results in the creation of compound 9, which has two chiral carbons. This is due to the use of the aluminum catalyst, which had been previously synthesized. The catalyst is chiral, which induces chirality in the product. The

catalyst performs two functions in the synthesis. First, it activates the benzaldehyde by complexing with the oxygen of the benzaldehyde, making the carbon more positive. Secondly, because of the size of the catalyst it creates steric hindrance so the oxazole is only able to attack from one side (Figure 20), leading to the stereochemistry of the product. Because the oxazole is protected with a methoxyphenyl, which also creates some steric hinderence, there is only one possible conformation that nucleophilic attack can occur in. This leads to the creation of the two chiral carbons in the product.

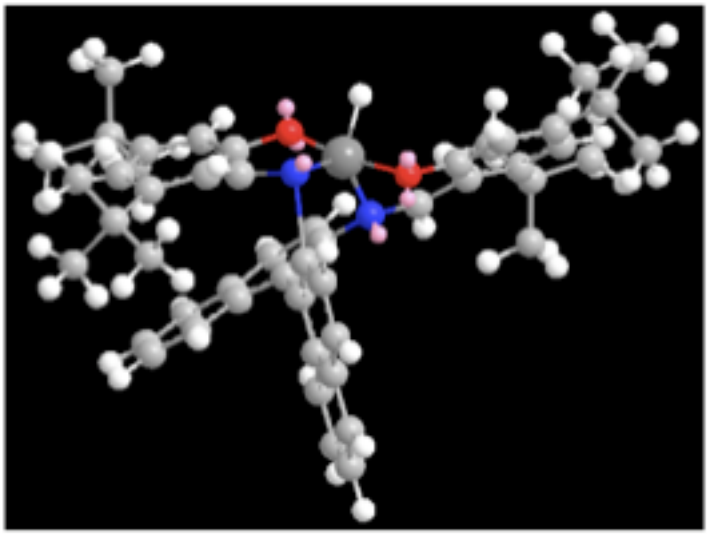

Figure 20: 3-D structure of aluminum catalyst (25). Because of its size the catalyst causes huge steric hindrance during attack of the benzaldehyde by the oxazole. The aluminum complexes with the benzaldehyde at the open area at the top of the molecule. Therefore the oxazole can only attack from the top because of the steric hindrance below.[20]

IV. Aldol Coupling

In the final step of the synthesis that was completed, compound 9 was reacted with compound 10 in the presence of the catalyst, dimethylaluminum chloride and lithium bis(trimethylsilyl)amide, a strong base (Figure 21). The lithium base deprotonates carbon 5 in the oxazoline ring of compound 9, making the carbon negatively charged, planar and nucleophilic. The aluminum catalyst complexes to the two carbonyl groups of compound 10, holding them in place and increasing the electrophilicity of the aldehyde carbon. Next, nucleophilic attack of the partially positive aldehyde carbon by the negative oxazoline carbon occurs. The double bond to the oxygen breaks leaving a hydroxyl group on the final product, 3-(4S-Methoxycarbonyl-2-p-methoxyphenyl-5S-phenyl-4,5-dihydro-oxazol-4-yl)-3S-hydroxy-2R-methyl-N,N-diethylpropionamide (11). Because the benzene of compound 9 is pointed down and the catalyst is holding compound 10 in place there can only be addition from the top of the oxazoline (Figure 22).[19,20, 29, 30]

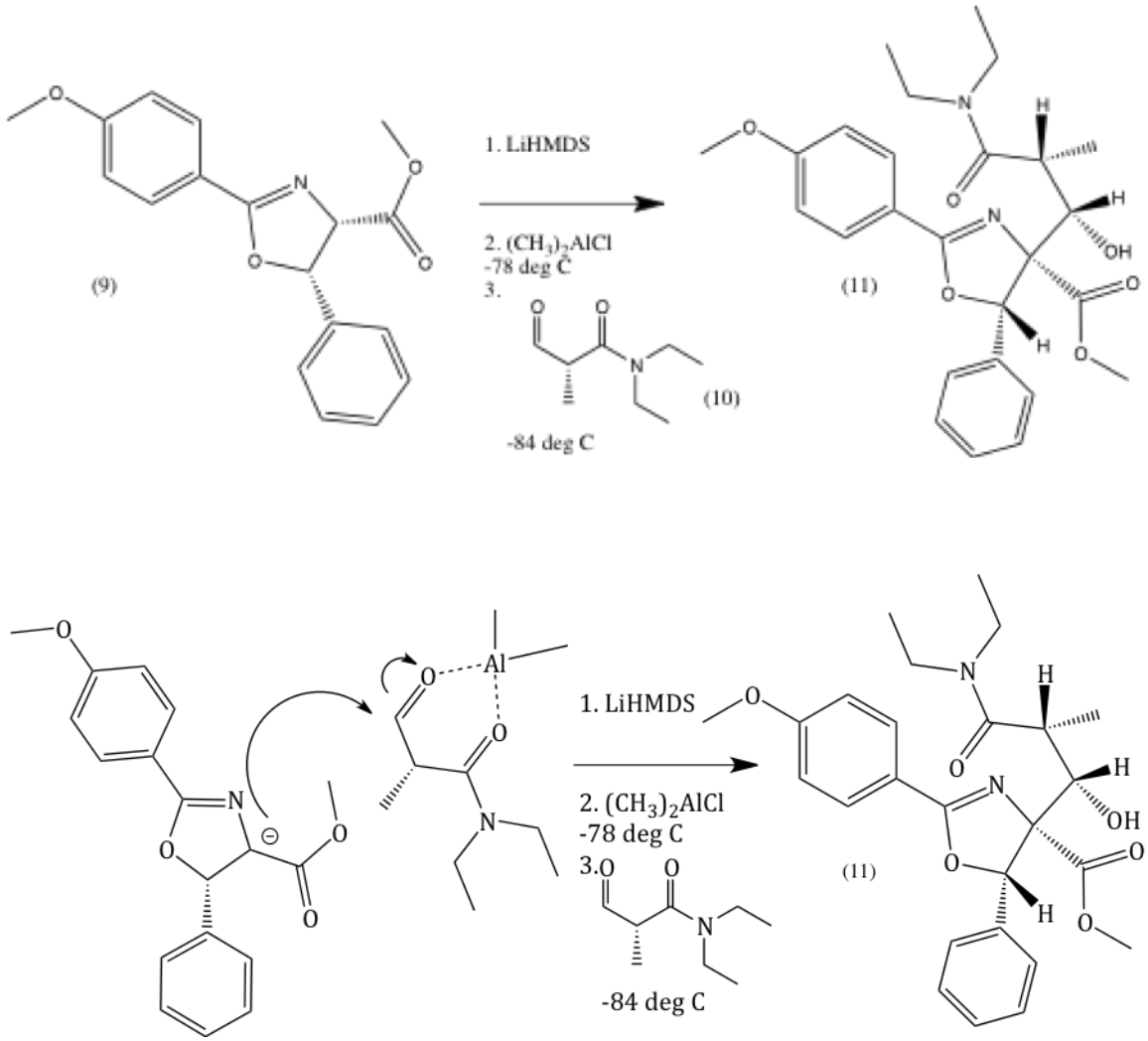

Figure 21: Mechanism of the synthesis of 3-(4S-Methoxycarbonyl-2-p-methoxyphenyl-5S-phenyl-4,5-dihydro-oxazol-4-yl)-3S-hydroxy-2R-methyl-N,N-diethylpropionamide (11).

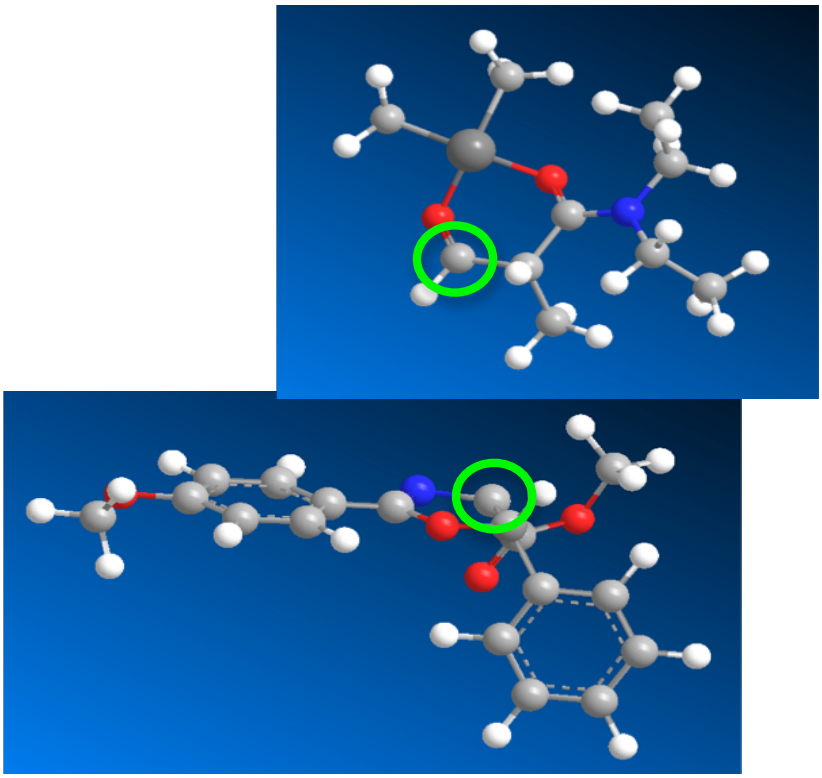

Figure 22: 3D structure of the reaction between compound 9 (bottom) and compound 10 (top). Compound 10 is complexed to the aluminum catalyst. As described above, because of steric hindrance caused by the phenyl of compound 9 and the catalyst there is only one possible conformation that this reaction can occur in, resulting in the stereospecific aldol product.

In this reaction compound 9, which has two chiral carbons and compound 10, which has one chiral carbon react to form compound 11, which has four chiral carbons. This is possible because of the catalyst, which controls the stereochemistry of the reaction via bidentate complexation to the amido aldehyde. This results in significant conformational constraint of the electrophilic aldehyde, which allows for the specific stereochemistry of compound 11.

Purification and identification of compound 11 has been challenging. The reaction resulted in four products, which were isolated via flash chromatography. The two predominant products are compound 11 and a corresponding stereoisomer (26) (Figure 23), in which the hydroxyl has opposite stereochemistry. Compound 26 is most likely the result of a loss of complexation between the catalyst and compound 10.

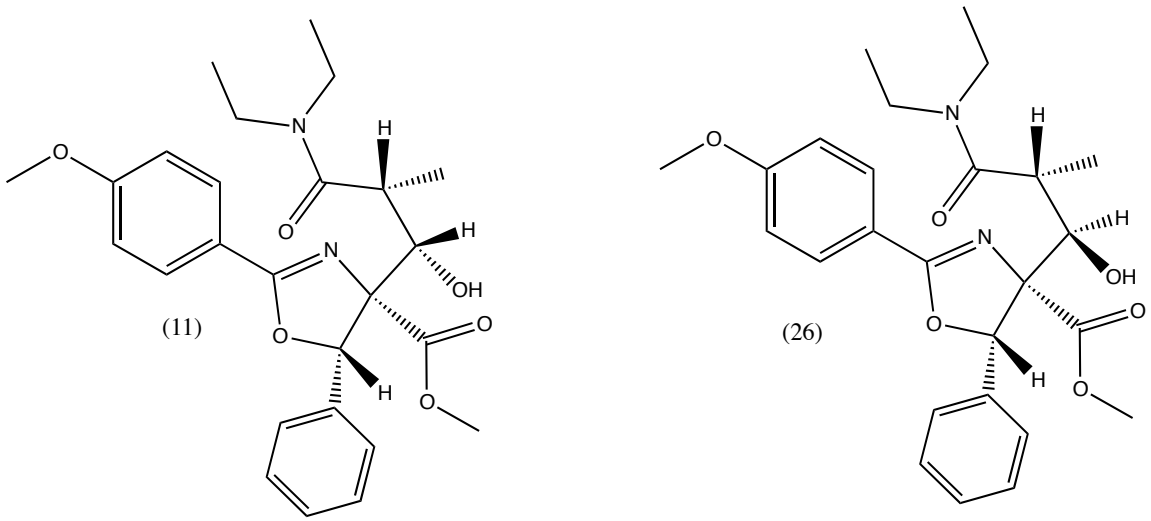

Figure 23: Compound 11 and its isomer (26).

Variation of reaction conditions have been previously studied for this reaction, including varying the temperature and doing the reaction without the catalyst. It was found that proper complexation between the aldehyde and catalyst only occurs at or below -85° C. Use of the achiral catalyst is also necessary for formation of the correct product. Because the starting materials are chiral, it is best to use an achiral catalyst to preserve stereochemistry in the product.

Comparing ^{1}H NMR spectra to previous spectra and modeling the two structures on Chem Draw 3D provides evidence that compound 11 was successfully synthesized. Compound 11 and 26 have different ^{1}H NMR spectra in respect to the placement of the hydroxyl proton. In one, the peak appears at 6.3 ppm and in the other at 4.3 ppm (Figure 24). Based on 3D images of the two different compounds in Chem Draw 3D there is a difference in orientation of the hydroxyl proton, which could account for this shift in the ^{1}H NMR (Figure 25). In compound 11 the hydrogen is pointing down toward the nitrogen of the ring. When molecular orbitals are included in the image it is clear that the hydrogen is directly over the molecular orbital of the nitrogen, where most of its electron density will be, allowing possible formation of a hydrogen bond between the two atoms. In compound 26 the hydrogen is pointing out, away from the nitrogen and when molecular orbitals are included it is not near any molecular orbitals and therefore would not be able to hydrogen bond. These differences lead to the shift in the peak in the ^{1}H NMR.

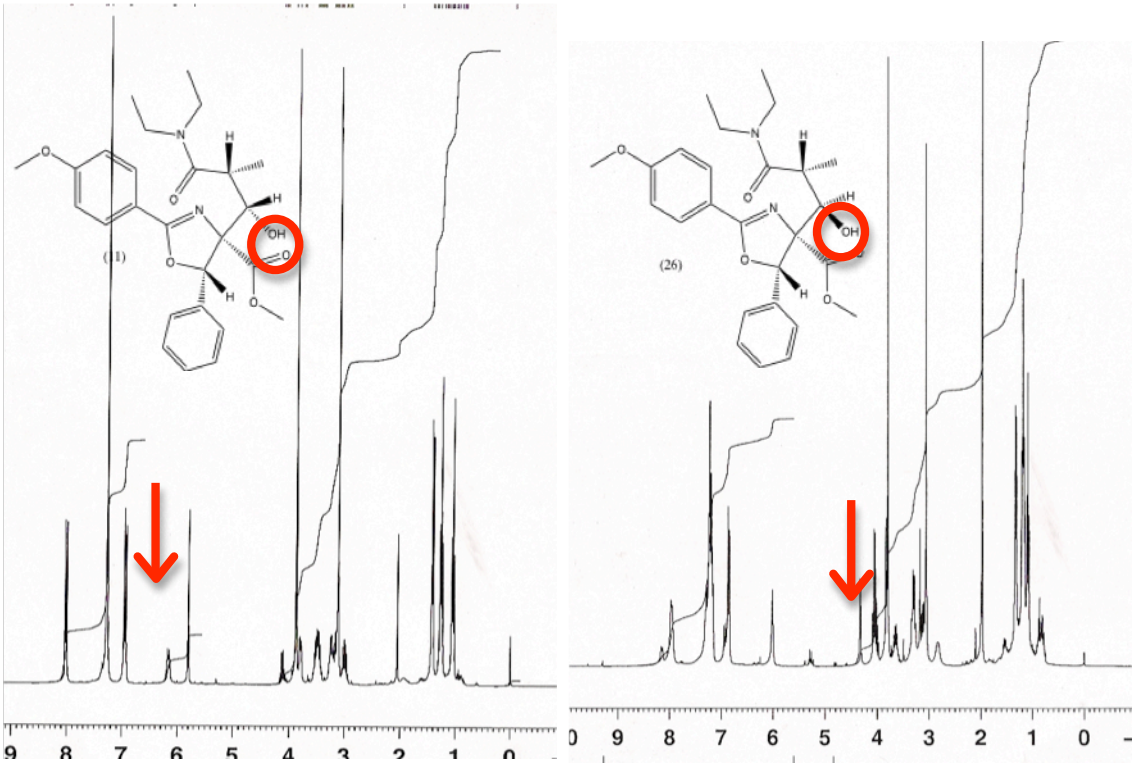

Figure 24: ^{1}H NMR of compound 11 and 26. Highlighted in red are the peaks for the corresponding hydroxyl protons.

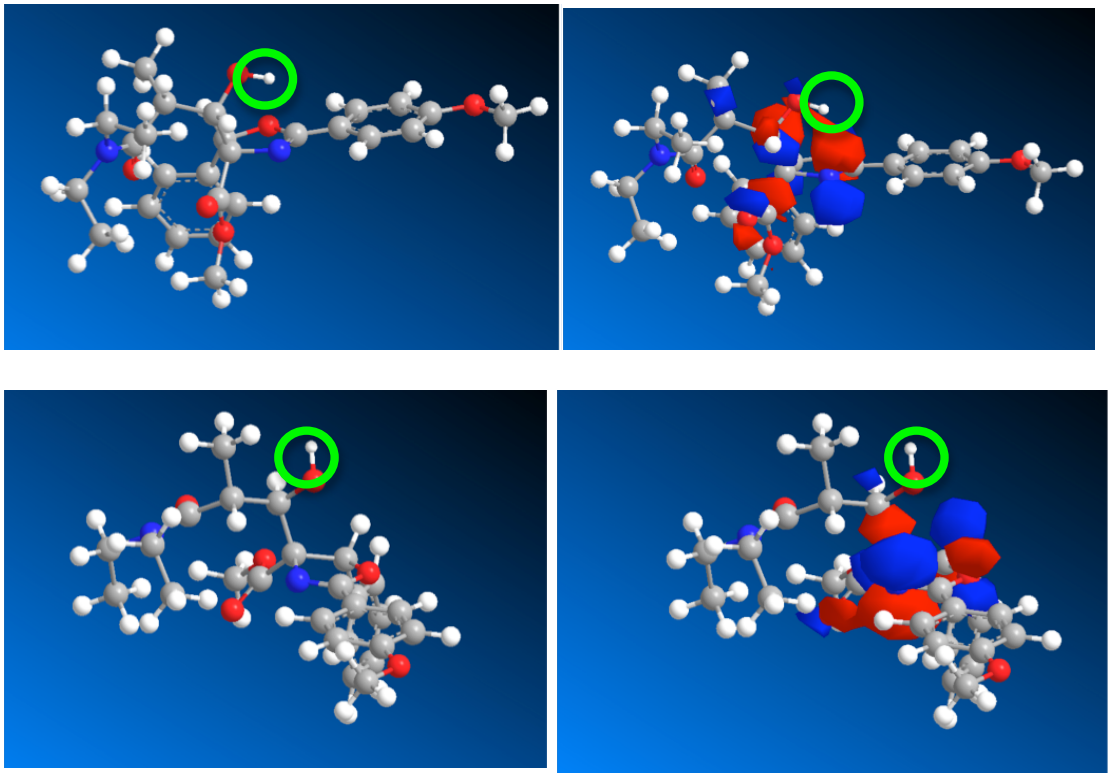

Figure 25: 3D structure of Compound 11 and Compound 26. Compound 11 is in the top row and compound 26 is in the bottom row. The hydroxyl proton is circled in green. Images to the right include predicted molecular orbitals from Chem Draw 3D.

Based on this data compound 11 was synthesized. Because of the complex stereochemistry methods could be employed to further prove the predicted stereochemistry is correct. First, NOESY NMR studies could be done; this is a 2D NMR technique, which shows which hydrogens are spatially close to each other. Second, one could obtain an x-ray crystal structure of the compound. Lastly more complex 3D modeling could be performed to conclude whether a hydrogen bond could form between the hydroxyl hydrogen and the nitrogen.

CONCLUSION

Significant progress toward the synthesis of the phenyl omuralide analog has been made and synthetic steps have been optimized. Further investigation into the stereochemistry of compound 11 needs to be performed. There are six more steps in the synthesis, which include the removal of protecting groups and closing of the β-lactone ring. Once finished the analog will be tested for inhibition of CPAF, which may lead to a lasting treatment for Chlamydia.

EXPERIMENTAL

General

Commercial reagents were purchased from Sigma-Aldrich, Alfa Aesar or Fischer and used without further purification. Air and water sensitive reactions were performed with oven-dried glassware fitted with rubber septa under a positive pressure of nitrogen. Thin-layer chromatography was performed on Merck 60-F_{254} pre-coated silica gel plates, which were visualized by exposure to ultraviolet light (254 nm). Column chromatography was performed using Sigma-Aldrich silica gel (60 Å, 70-230 mesh). Flash chromatography was performed using Biotage FLASH silica cartridges for the SPI system. ^{1}H NMR and ^{13}C NMR spectra were recorded using a Bruker 300 MHz WIN-NMR spectrometer with TMS as an internal standard. Mass spectra were measured with an Agilent 6890N Network GC System coupled with an electron impact Agilent 5937 Network Mass Selective Detector. The program "RAYANNE" ($T_{initial}$=120°C, T_{final}=325°C, rate=20°C/sec; split mode (inlet); mobile phase=He(g); constant flow mode, flow rate 1.0 mL/min; injection volume 1.0 uL, pressure 11.6 psi) was used for GC/MS analysis. Catalytic hydrogenation was performed in a Parr Instrument Company Pressure Reaction Apparatus.

Synthesis

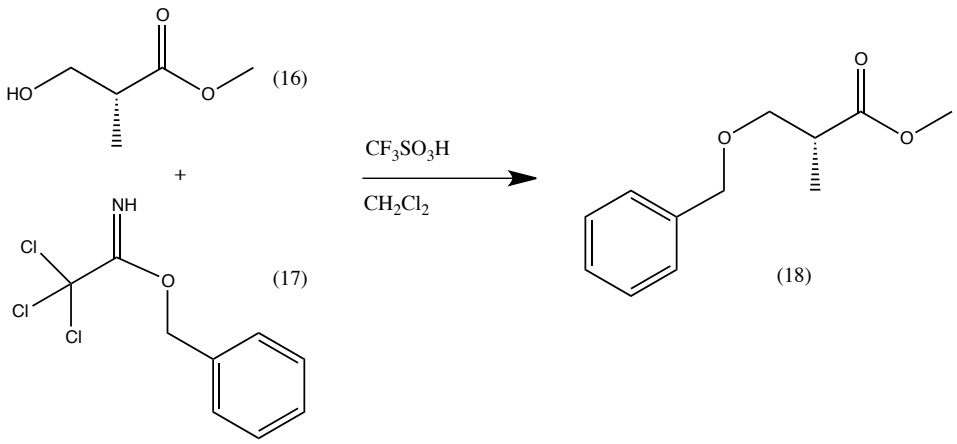

Methyl (2R)-3-benzyloxy-2-methylpropionate (18). Methyl (2R)-3-hydroxy-2-methylpropionate (5.17 g, 43.8 mmol) was dissolved in 100 mL of cyclohexane and 50 mL of CH_2Cl_2. Benzyl 2,2,2-trichloroacetimidate (13.54 g, 53.7 mmol) was added to the reaction mixture. Triflic acid (0.405 mL, 0.696 g, 4.64 mmol) was added slowly to the mixture. The reaction mixture was stirred at room temperature for 24 hours. The resulting suspension was filtered and the filtrant was washed well with CH_2Cl_2, which was added to the original filtrate. The solvents were then washed with water (2x100 mL), saturated $NaHCO_3$ (2x50 mL) and brine (2x25 mL). The organic fraction was dried over Na_2SO_4 and the solvent was evaporated. Addition of hexane (25 mL) resulted in no precipitation of trichloroacetamide, so the solvent was evaporated. Purification was accomplished by chromatography (silica gel, 10% EtOAc in hexane) to give a slightly yellow product (8.36 g, 40.1 mmol, 91.6%). Purification was not a complete success as there were still many contaminants in the GC/MS, but GC/MS analysis showed product was dominant in the mixture.

GC/MS spectrum (Appendix 1): Mass ion: 208 m/z. The product was used without further purification.

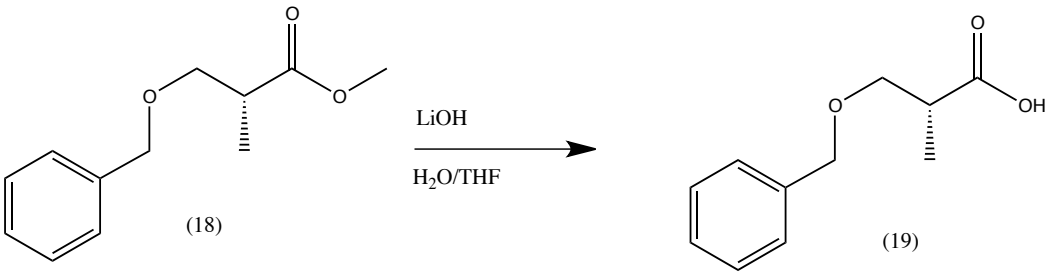

(2R)-3-Benzyloxy-2-methylpropionic acid (19). Methyl (2R)-3-benzyl-2-methylpropionate (8.36 g, 40.1 mmol) was added to 100 mL of a 1:1 mixture of THF and water, and the mixture was cooled on ice. $LiOH{\cdot}H_2O$ (2.53 g, 106 mmol) was added in small portions over 10 minutes and the reaction was stirred at 4 ^oC. After 24 hours at 4 ^oC, $NaHCO_3$ (4.97 g, 59.2 mmol) and water (22 mL) were added and the THF was removed under vacuum. The aqueous solution was washed with CH_2Cl_2 (3x20 mL) and then acidified to ~pH1 with 6M HCL (~20 mL). The acidified suspension was extracted with CH_2Cl_2 (3x40 mL). The organic fraction was dried over Na_2SO_4 and the solvent was removed under vacuum to give a nearly pure, slightly yellow oil (5.18 g, 26.7 mmol, 66.6%). ^1H NMR ($CDCl_3$) (Appendix 2) δ 11.75 (s, 1H, OH) 7.4-7.25 (m, 5H, Ph), 4.5 (s, 2H, benzyl CH_2), 3.7 (m, 1H, propionyl CH_2a), 3.6 (dd, 1H, propionyl CH_2b), 2.8 (m, 1H, propionyl CH), 1.3 (d, 3H, propionyl CH_3). ^{13}C NMR ($CDCl_3$) (Appendix 3) δ 181.61 (ipso, C=OOH), 138.37 (ipso), 128.86,

128.16, and 128.11 (aromatic), 73.63 (propionyl CH_2), 72.02 (benzyl CH_2), 40.61 (propionyl CH), 14.22 (propionyl CH_3).

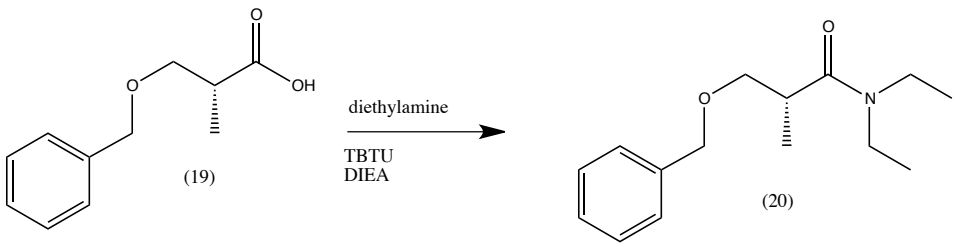

3-Benzyloxy-N,N-diethyl-2-(R)-methylpropionamide (20). 3-Benzyloxy-2-(R)-methylpropionic acid (5.18 g, 26.7 mmol) was dissolved in anhydrous CH_3CN (31 mL) and the solution was cooled on ice for 15 min. Diethylamine (3.27 mL, 2.30 g, 31.4 mmol), TBTU (9.34 g, 29.1 mmol), and diisopropylethylamine (9.27 mL) were added to the solution, in that order. The solution was stirred on ice for 2 hours. Ether (35 mL) and water (140 mL) were added to the reaction, and the ether was collected. The aqueous layer was extracted with additional ether (2x35 mL). The combined organic layers were washed with 5% HCl (2x15 mL) and then saturated $NaHCO_3$ (25 mL). The organic layer was dried with Na_2SO_4 and the solvent was evaporated to give a nearly pure product (5.14 g, 20.6 mmol, 77%). ^1H NMR ($CDCl_3$) (Appendix 4) δ 7.4-7.2 (5H, Ph), 4.5 (dd, 2H, benzyl Ch_2), 3.7 (dd, 1H, propionyl CH_2), 3.5-3.2 (m, 5H, amide CH_2a and CH_2b and propionyl CH_2), 3.0 (apparent hextet, 1H, propionyl methine), 1.2-1.1 (t, 9H, ethyl CH_3's and propionyl CH_3). ^{13}C NMR ($CDCl_3$) (Appendix 5) δ 174.61 (ipso, C=O), 138.9 (ipso), 128.65, 128.40 and 127.79 (Ph),

73.94 and 73.60 (propionyl CH_2 and benzyl CH_2), 42.33 and 40.85 (ethyl CH_2's) 36.86 (propionyl methine), 15.31 and 13.50 (ethyl CH_3's).

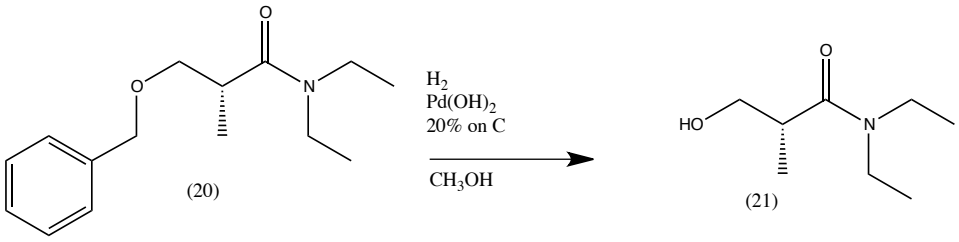

N,N-Diethyl-3-hydroxy-2-(R)-methylpropionamide (21). Palladium hydroxide (20% on C, 0.35 g) was added to a hydrogenation flask. Methanol (5 mL) was slowly added to the flask. 3-Benzyloxy-N,N-diethyl-2-(R)-methylpropionamide (5.14 g, 20.6 mmol) was dissolved in 10 mL of methanol, which was then added to the reaction mixture. Additional methanol (50 ml) was added to the reaction flask and the flask was connected to the hydrogenator. The reaction was placed under H_2 (10 PSI). After 48 hours, the reaction mixture was gravity filtered and the solvent was evaporated to give the alcohol as a nearly pure colorless oil (3.38 g, 21.3 mmol, 100%). The oil was used in the next reaction without further purification. ^{1}H NMR ($CDCl_3$) (Appendix 6) δ 3.8 (s, 1H, OH), 3.7 (dd, 1H, propionyl CH_2-a) 3.6 (dd, 1H, propionyl CH_2-b) 3.5-3.2 (m, 4H, ethyl CH_2's), 2.8 (tq, 1H, methine CH), 1.2-1.1 (9H, t, 3H, ethyl CH_3a, d, 3H, propionyl CH_3, t, 3H, ethyl CH_3b). ^{13}C NMR ($CDCl_3$) (Appendix

7) δ 175.87 (C=O), 65.34 (propionyl C3), 42.29 and 40.56 (ethyl methylenes), 38.05 (methine), 14.98, 14.65, and 13.28 (methyls).

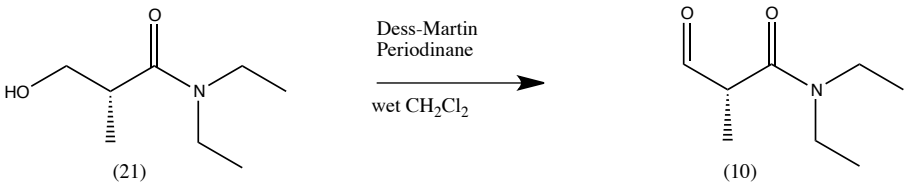

N,N-Diethyl-2-(R)-methyl-3-oxopropionamide (10). N,N-Diethyl-3-hydroxy-2-(R)-methylpropionamide (1.25 g, 7.85 mmol) was dissolved in wet CH_2Cl_2 (prepared by stirring 50ml CH_2Cl_2 with about 2 mL of water for 48 hours). Dess-Martin periodinane (from Sigma Aldrich) (5 g, 11.7 mmol) was added slowly over 8 minutes. The reaction mixture was stirred at room temperature for a total of 1 hour. The reaction was then cooled in an ice bath and quenched by the addition of a cold (~4 ^{0}C) solution of $Na_2S_2O_3 \cdot 5H_2O$ (18 g, 113 mmol) and $NaHCO_3$ (3.96 g, 47.1mmol) dissolved in 102 mL of water. The mixture was stirred on ice for 10 minutes, ether (75 mL) was added, and the mixture was stirred vigorously at RT for an additional 10 minutes. The organic layer was collected and the aqueous layer was washed with 1:2 CH_2Cl_2:ether (2x20 mL). The combined organic layers were washed with brine (2x25 mL) and then dried over Na_2SO_4. Evaporation of the solvent gave the aldehyde as nearly pure colorless oil (0.68 g, 4.33 mmol, 55%). The aldehyde should be stored under nitrogen as a solution in CH_2Cl_2 at 0 ^{o}C.

^{1}H NMR ($CDCl_3$) (Appendix 8) δ 9.7 (1H, aldehyde H), 3.7-3.3 (m, 5H, ethyl CH_2's and CH),1.5 (d, 3H, propionyl CH_3), 1.1-1.25 (6H, t, 3H, ethyl CH_3a, t, 3H, ethyl CH_3b). ^{13}C NMR ($CDCl_3$) (Appendix 9) δ 199.85 (C=O), 169.49 (ipso, C=O) 50.05 (propionyl C3), 42.51 and 40.77 (ethyl methylenes), 15.14, 13.41, and 12.92 (methyl's).

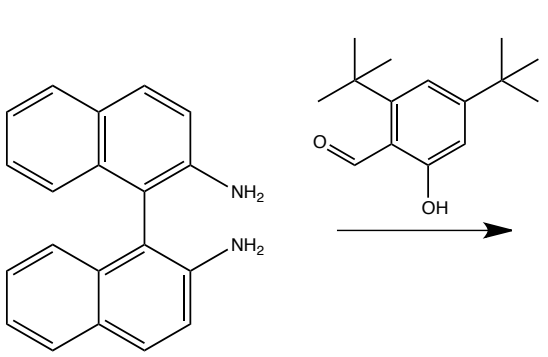

(23)

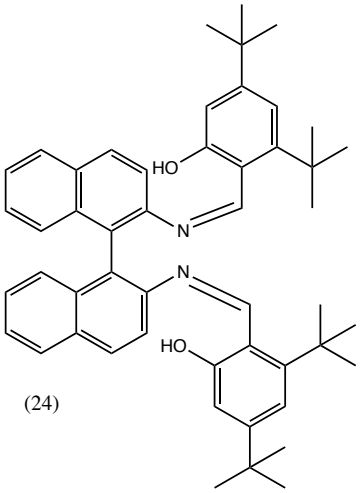

(24)

(*R*)-2,2'-Bis(3,5-di-*tert*-butyl-2-hydroxybenzylideneamino)-1,1'-binaphthyl (24). 1,1-Binaphthyl-2,2'-diamine (1.04 g, 3.66 mmol) and 3,5-di-*tert*-butyl-2-hydroxybenzaldehyde (1.72 g, 7.34 mmol) were added to 122 mL of absolute ethanol. The solution was heated at reflux for 21 hours. Water was added to the boiling solution until a persistent precipitation was achieved. The mixture was then removed from heat and allowed to cool to RT. The product was isolated by filtration as a yellow powder. The product was purified by column chromatography (20:1 hexane:ethyl acetate) and was the first product off the column. Solvent was removed under vacuum to give a nearly pure yellow powder (1.23 g, 1.72 mmol, 47%). Purity was evaluated by TLC in 15:1 hexane:ethyl acetate. ^{1}H NMR ($CDCl_3$) (Appendix 10) δ 8.8 (s, 2H, N=CH), 8.2 (6H, binap proton positions 4,4',5,5',8, 8'), 7.7 (2H, binap

proton positions 3, 3'), 7.5 (4H, binap protons positions 6,6',7,7'), 7.2 (4H, phenyl), 7.0 (2H, OH), 1.4-1.2 (36H, 12 methyls).

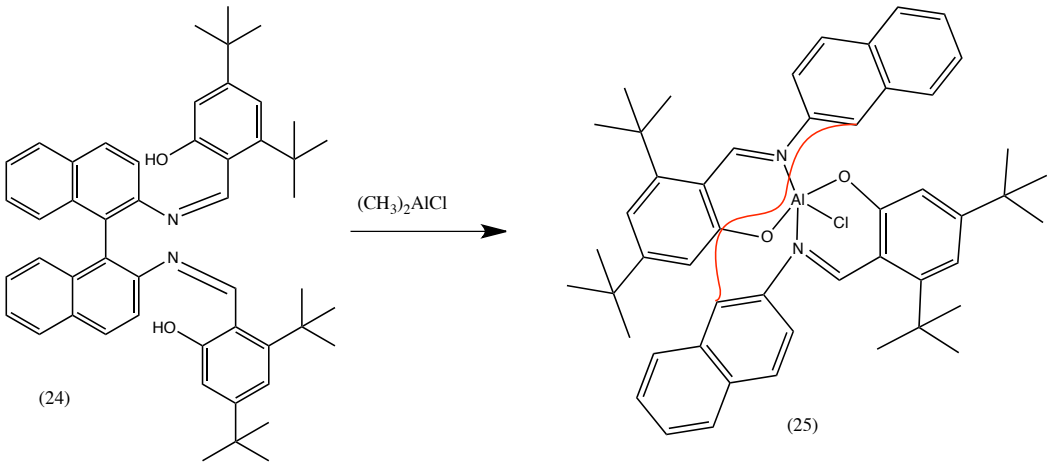

(*R*)-2,2'-Bis(3,5-di-*tert*-butyl-2-hydroxybenzylideneamino)-1,1'-binaphthyl aluminum chloride (25). (*R*)-2,2'-Bis(3,5-di-*tert*-butyl-2-hydroxybenzylideneamino)-1,1'-binaphthyl (1.21 g, 1.69 mmol) was dissolved in CH_2Cl_2 (13 mL) under N_2. The solution was cooled in an ice bath. Dimethylaluminum chloride (0.1554 g, 0.22 ml, 1.68 mmol) was added by syringe slowly to the reaction. The reaction was left to warm to RT overnight, under N_2. After 20 hours, the solvent was removed under vacuum to give a yellow powder (1.53 g, 1.96 mmol, 86%), which can be stored at RT until needed.

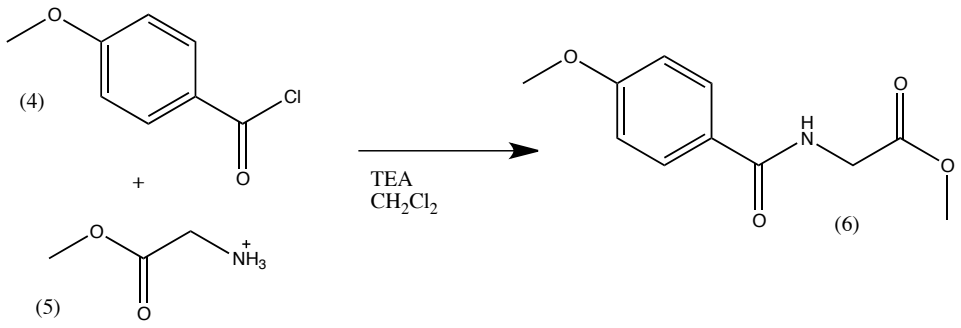

N-4-Methoxybenzoylglycine methyl ester (6). Glycine methyl ester hydrochloride (18.12 g, 144 mmol) was dissolved in CH_2Cl_2 (487 mL) and the mixture was cooled on ice. Triethylamine (32 mL) was added to the mixture. The mixture was stirred for 10 minutes on ice. 4-Methoxybenzoyl chloride (25 g, 147 mmol) was added to the mixture slowly while stirring. The sides of the flask were rinsed with additional CH_2Cl_2 (40 mL). The reaction was removed from the ice bath and stirred at room temperature for 17 hr. The reaction mixture was then washed with water (2x50 mL), 5% HCl (2x50 mL), and saturated aqueous $NaHCO_3$ (50 mL) and then dried over Na_2SO4. Evaporation of the solvent gave an off-white solid. The solid was dissolved in 80 mL of warm CH_3OH. The mixture was kept warm while adding water (100 mL). The mixture was removed from heat and allowed to cool to room temperature. The product was allowed to continue to crystallize at 4°C for 24 hours. The product formed needle-like colorless crystals (24 g, 107.5 mmol, 74.7%). ^1H NMR ($CDCl_3$) (Appendix 11) δ 7.8 (d, 2H, Ph), 6.9 (d, 2H, Ph), 6.65 (br, 1H, NH), 4.3 (d, 2H, CH_2), 3.8 (s, 3H, CH_3-OAr), 3.8 (s, 3H, ester-CH_3).

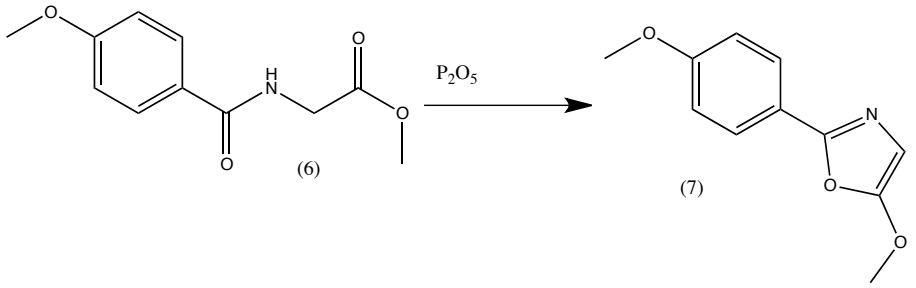

5-Methoxy-2-p-methoxyphenyloxazole (7). N-4-Methoxybenzoylglycine methyl ester (11.46 g, 51.4 mmol) was dissolved in $CHCl_3$ (105 mL). Phosphorus pentoxide (46.5 g, 328 mmol) was added. The reaction was heated to reflux. As the reaction progressed, solid formed in the reaction flask, inhibiting the reaction. The solid residues were broken up several times for the first 8 hours of the reaction. After 22 hours, the reaction was removed from heat and cooled to ~4 ^{0}C. Once cool the reaction mixture was poured into a 4 ^{0}C solution of NaOH (40.4 g, 1.01 mol, in 400 mL of water). The reaction flask was rinsed with additional $CHCl_3$ (100 ml), which was added to the NaOH solution. The organic layer was separated and the aqueous layer was washed with $CHCl_3$ (2x20 mL). The combined organic layers were washed with 5% HCl (2x40 mL) and then saturated $NaHCO_3$ (50 mL). The organic layer was dried over Na_2SO_4 and the solvent was evaporated leaving a yellow solid. Column chromatography (silica, 1:3 EtOAc:hexane) gave a nearly pure product (second product off column). The product was recrystallized in 1:3 EtOAc:hexane, giving large colorless crystals (4.21 g, 20.5 mmol, 40%): ^{1}H NMR ($CDCl_3$) (Appendix 12) δ 7.9 (d, 2H, Ph), 7.0 (d, 2H, Ph), 6.2 (s, 1H, oxazole H), 4.0 (s, 3H, Oxa-OCH_3), 3.8 (s, 3H, ArO-CH_3). ^{13}C NMR ($CDCl_3$) (Appendix 13) δ 161.18 and 160.92 (ipso, C=O and

oxazole-C2), 153.19 (ipso, phenyl)127.39 (OAr-meta), 120.76 (ipso, OAr-para), 114.53 (OAr-ortho), 99.70 (oxazole-C5), 59.07 (CH_3-O-oxazole), 55.75 (CH_3-OAr).

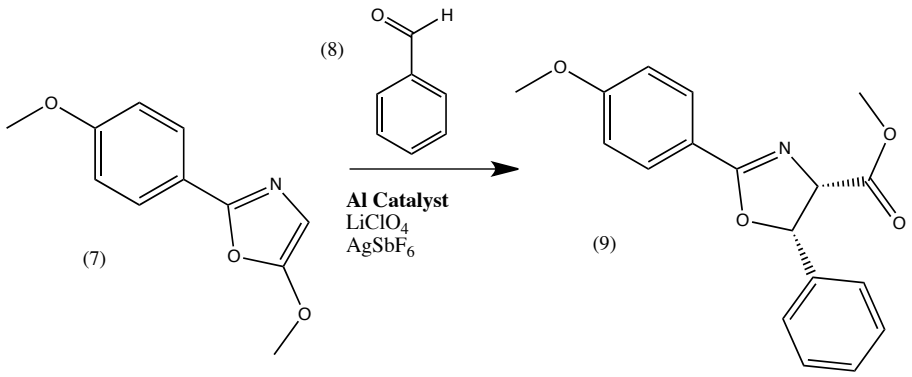

(4R,5S)-2-p-Methoxyphenyl-5-phenyl-4,5-dihydrooxazole-4-carboxylic Acid Methyl Ester (9). Powdered 3Å molecular sieves (2.0 g) were dried overnight at 120 ^{0}C in the reaction flask. The reaction flask was flushed with N_2 and then the aluminum chloride complex of (R)-2,2'-s(3,5-Di-tert-butyl-2-hydroxybenzylideneamino)-1,1'-binaphthyl (0.411 g, 0.53 mmol), $LiClO_4$ (0.74 g, 7.0 mmol), $AgSbF_6$ (0.34 g, 1.0 mmol), and 5-Methoxy-2-p-methoxyphenyloxazole (2.05 g, 10.0 mmol) were added to the reaction flask. The flask was flushed further with N_2. Anhydrous toluene (20 mL) was added to the flask via syringe. The reaction mixture was stirred at RT. Benzaldehyde (1.27 g, 1.22 mL, 12.0 mmol) was added to the reaction flask via syringe. The reaction was stirred at RT for 24 hours. The reaction mixture was filtered through a short bed of silica gel, and the silica gel was washed with EtOAc. The solvent was removed under vacuum to give a yellowish,

orange oil. Flash chromatography (silica, 5% - 60% EtOAc in hexane), followed by removal of the solvent gave a pale yellow solid. The product was dissolved in a 1:3 mixture of EtOAc:hexanes and allowed to recrystallize at 4° C overnight. This gave pure yellow needle-like crystals (0.68 g, 2.19 mmol, 22%). ^{1}H NMR ($CDCl_3$) (Appendix 14) δ 8.1 (d, 2H, CH_3O-Ph-H), 7.4-7.2 (m, 5H, Ph), 6.9 (d, 2H, CH_3O-Ph-H), 5.9, (d, 1H, oxa-H5), 5.3 (d, 1H, oxa-H4), 3.9 (s, 3H, Ar-OCH_3), 3.2 (s, 3H, ester-CH_3).

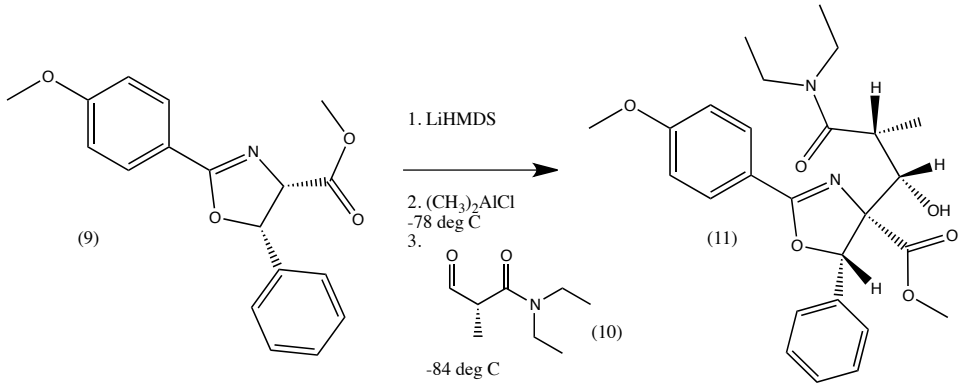

3-(4S-Methoxycarbonyl-2-p-methoxyphenyl-5S-phenyl-4,5-dihydro-oxazol-4-yl)-3S-hydroxy-2R-methyl-N,N-diethylpropionamide (11). (4R,5S)-2-p-Methoxyphenyl-5-phenyl-4,5-dihydrooxazole-4-carboxylic acid methyl ester (0.34 g, 2.19 mmol) was placed in an N_2 flushed flask. Dry THF (7 mL) was added to the flask via syringe. The mixture was cooled in an EtOAc/dry ice bath (temperature ~ -75^0 C). LiHMDS (1M in THF, 1.075 mL, 1.07 mmol) was added to the reaction flask via syringe over 3 minutes. The reaction was stirred at ~ -75 ^{0}C for 40 minutes. Dimethylaluminum chloride (0.254g, 0.362mL, 2.75 mmol) was added slowly over 3 minutes via syringe. The reaction was stirred for 40 minutes at -75 ^{0}C. Liquid N_2

was then added to the EtOAc/dry ice bath to decrease the temperature to -85 ^{0}C. The temperature was left to stabilize for 10 minutes. Next, 3-Oxo-2R-methyl-N,N-diethyl-propionamide (0.214g, 1.36 mmol) which had previously been placed in an oven dried flask and flushed with N_2 was added in 0.5 mL of dry THF via syringe. The flask, which had held the aldehyde, was rinsed with additional THF (3x0.5 mL), which were added to the reaction. The reaction was stirred at -84 ^{0}C for 15 minutes, and then allowed to warm slowly (5 hours) to about -20 ^{0}C. The reaction mixture was then cooled back down to -60 ^{0}C and quenched by the addition of saturated NH_4Cl (0.5 mL) via syringe. The resulting slurry was warmed to RT and poured into a mixture of saturated NH_4Cl (10 mL) and a 1:1 mixture of EtOAc: hexane (2.5 mL). The reaction flask was rinsed with water (2x2 mL) and additional EtOAc:hexane (2x1 mL). HCl (10% solution, 2 mL) was added to the mixture. The organic layer was removed. The aqueous layer was washed with 1:1 EtOAc:hexane (2x10 mL). The combined organic layers were washed with 1M HCl (10 mL), water (10 mL), saturated $NaHCO_3$ (10mL), and brine (10 mL). The organic layer was then dried over Na_2SO_4. Flash chromatography (silica, 25%-50% EtOAc in hexane) gave the desired aldol product as the last major product from the column (0.26 g, 0.556 mmol, 26%) ^{1}H NMR ($CDCl_3$) (Appendix 15) δ 8.1 (d, 2H, CH3OAr-H), 7.3 (s, 5H, Ar-H), 6.9 (d, 2H, CH_3OAr-H), 6.2 (d, 1H, OH), 5.8 (s, 1H, oxa-H-5), 3.9 (s, 3H, Ph-OCH_3), 3.8 (d, 1H, CH-O(H)), 3.5 (dq, 2H, N-CH-a), 3.25 (dd, 1H, CH-(CH_3)), 3.15 (d, 1H, N-CH-b-1) 3.1 (s, 3H, ester CH_3), 3.0 (dq, 1H, N-CH-b-2), 1.4 (d, 3H, prop-CH_3), 1.25 (t, 3H, Et-CH_3-1), 1.05 (t, 3H, Et-CH_3-2).

REFERENCES

1. Mayer, G., Bacteriology-Chapter 20 Chlamydia and Chlamydophila. In *Microbiology and Immunology On-line*, University of South Carolina School of Medicine: **2010**.

2. Centers for Disease Control and Prevention. Sexually Transmitted Diseases: Chlamydia CDC Fact Sheet. http://www.cdc.gov/std/chlamydia/stdfact-chlamydia.htm (accessed June 20, 2010).

3. Chlamydia. In *A.D.A.M. Medical Encyclopedia*, PubMed Health: **2011**.

4. Belland, R. J.; Zhong, G.; Crane, D. D.; Hogan, D.; Sturdevant, D.; Sharma, J.; Beatty, W. L.; Caldwell, H. D., Genomic transcription profiling of the developmental cycle of chlamydia trachomatis. *Proc. Natl. Acad. Sci*. **2003**, (100), 8478-8483.

5. Christian, J.; Vier, J.; Paschen, S.; Hacker, G., Cleavage of the NF-kB Family Protein p65/RelA by the Chlamydial Protease-like Activity Factor (CPAF) Impairs Proinflammatory Signaling in Cells Infected with Chlamydiae. *Journal of Biological Chemistry* **2010**, 285, (53), 41320-41327.

6. Huang, Z.; Feng, Y.; Chen, D.; Wu, X.; Huang, S.; Wang, X.; Xiao, X.; Li, W.; Huang, N.; Gu, L.; Zhong, G.; Chai, J., Structural Basis for Activation and Inhibition of the Secreted Chlamydia Protease CPAF. *Cell Host & Microbe.* **2008**, 4, 529-542.

7. Dong, F.; Sharma, J.; Xiao, Y.; Zhong, Y.; Zhong, G., Intramolecular Dimerization is Required for the Chlamydia-Secreted Protease CPAF to Degrade Host Transcriptional Factors. *Infect. Immun.* **2004**, 72, (7), 3869-3875.

8. Zhong, G.; Fan, P.; Ji, H.; Dong, F.; Huang, Y., Identification of a Chlamydial Protease–Like Activity Factor Responsible for the Degradation of Host Transcription Factors. *Journal of Experimental Medicine* **2001**, 193, (8), 935-942.

9. Pirbhai, M.; Dong, F.; Zhong, Y.; Pan, K. Z.; Zhong, G., The secreted protease factor CPAF is responsible for degrading pro-apoptotic BH3-only proteins in Chlamydia trachomatic-infected cells. *J. Cell Biol* **2006**, (182), 117-127.

10. Christian, J.; Vier, J.; Paschen, S.; Hacker, G., Cleavage of the NF-kB Family Protein p65/RelA by the Chlamydial Protease-like Activity Factor (CPAF) Impairs Proinflammatory Signaling in Cells Infected with Chlamydiae. *Journal of Biological Chemistry* **2010**, 285, (53), 41320-41327.

11. Yu, H.; Schwarzer, K.; Forster, M.; Kniemeyer, O.; Forsbach-Birk, V.; Straube, E.; Rodel, J., Role of high-mobility group box 1 protein and poly(ADP-ribose) polymerase 1 degradation in Chlamydia trachomatis-induced cytopathicity. *Infect. Immun.* **2010**, (78), 3288-3297.

12. Sun, J.; Kintner, J.; Schoborg, R. V., The host adherens junction molecule nectin-1 is downregulated in Chlamydia trachomatis-infected genital epithelial cells. *Microbiology* **2008**, (154), 1290-1299.

13. Paschen, S. A.; Christian, J. G.; Vier, J.; Schmidt, F.; Welch, A.; Ojcius, D. M.; Hacker, G., Cytopathicity of Chlamydia is largely reproduced by expression of a single chlamydial protease. *J. Cell Biol* **2008**, (281), 31495-31501.

14. Jorgensen, I.; Bednar, M. M.; Amin, V.; Davis, B. K.; Ting, J. P. Y.; McCafferty, D. G.; Valdivia, R. H., The Chlamydia Protease CPAF Regulates Host and Bacterial Proteins to Maintain Pathogen Vacuole Integrity and Promote Virulence. *Cell Host & Microbe* **2011**, (10), 21-32.

15. Corey, E. J.; Li, W.-D.; Nagamitsu, T.; Fenteany, G., The Structural Requirements for Inhibition of Proteasome Function by the Lactacystin-Derived B-Lactone and Synthetic Analogs. *Tetrahedron* **1999**, 55, 3305-3316.

16. Reddy, L. R.; Fournier, J.-F.; Reddy, B. V. S.; Corey, E. J., An Efficient, Stereocontrolled Synthesis of a Potent Omuralide-Salinosporin Hybrid for Selective Proteasome Inhibition. *J. Am. Chem. Soc* **2005**, (127), 8974-8976.

17. Corey, E. J.; Li, W.; Nagamitsu, T., An Efficient and Concise Enantioselective Total Synthesis of Lactacystin. *Angew. Chem. Int. Ed.* **1998,** 37, (12), 1676-1679.

18. Corey, E. J.; Li, W.-D. Z., Total Synthesis and Biological Activity of Lactacystin, Omuralide and Analogs. *Chem. Pharm. Bull* **1999**, 47, 1-10.

19. Soucy, F.; Grenier, L.; Behnke, M. L.; Destree, A. T.; McCormack, T. A.; Adams, J.; Plamondon, L., A Novel and Efficient Synthesis of a Highly Active Analogue of clasto-Lactacystin B-Lactone. *J. Am. Chem. Soc* **1999**, 121, 9967-9976.

20. Haines, D. R. Sabbatical Report Experimental Procedures, Duke University 2008-2009.

21. White, J. D.; Kawasaki, M., Total synthesis of (+)-latrunculin A, an ichthyotoxic metabolite of the sponge Latrunculia magnifica and its C-15 epimer *J. Org. Chem.* **1992,** 50, (20), 5292-5300.

22. Han, S.-Y.; Kim, Y.-A., Recent development of peptide coupling reagents in organic synthesis. *Tetrahedron* **2004,** 60, (11), 2447-2467.

23. Montalbetti, C. A. G. N.; Falque, V., Amide bond formation and peptide coupling. *Tetrahedron* **2005,** 61, (46), 10827-10852.

24. Meyer, S. D.; Schreiber, S. L., Acceleration of the Dess-Martin Oxidation by Water. *J. Org. Chem.* **1994,** 59, (24), 7549-7552.

25. Smith, M. B.; March, J., *March's Advanced Organic Chemistry*. 6 ed.; John Wiley & Sons Inc: Hoboken, 2007.

26. Dess-Martin Oxidation. In Organic Chemistry Portal: 2011. <http://www.organic-chemistry.org/namedreactions/dess-martin-oxidation.shtm>.

27. Evans, D. A.; Janey, J. M.; Magomedov, N.; Tedrow, J. S., Chiral salen-aluminum complexes as catalysts for enantioselective aldol reactions of aldehydes and 5-alkoxyoxazoles: an efficient approach to the asymmetric synthesis of syn and anti alpha-hydroxy-alpha-amino acid derivatives. *Angewandte Chemie International Edition* **2001,** 40, (10), 1884-1888.

28. Bentama, A.; Hadrami, E. M. E.; Hallaoui, A. E.; Elachqar, A.; Lavergne, J., Synthesis of new alpha-heterocyclic alpha-aminoesters. *Amino Acids* **2003,** 24, (4), 423-426.

29. L'abbe, G.; Ilisiu, A. M.; Dehaen, W.; Toppet, S., Synthesis and thermolysis of 5-azido-4-formyloxazoles. *Perkin Transactions 1: Organic and Bio-Organic Chemistry (1972-1999)* **1993**, (19), 2259-2261.

30. Suga, H.; Shi, X.; Ibata, T., Steroselective Synthesis of 2-Oxazoline-4-carboxylates through Lewis Acid-catayzed Formal [3 + 2] Cycloaddition of 5-Alkoxyoxazoles with Aldehydes: Catalytic Effect of Methylaluminum B-Binaphthoxide on Cis-Selectivity. *J. Org. Chem.* **1993**, (58), 7397-7405.

INDEX OF APPENDICES

Appendix 1: Mass spectrum of compound 18.

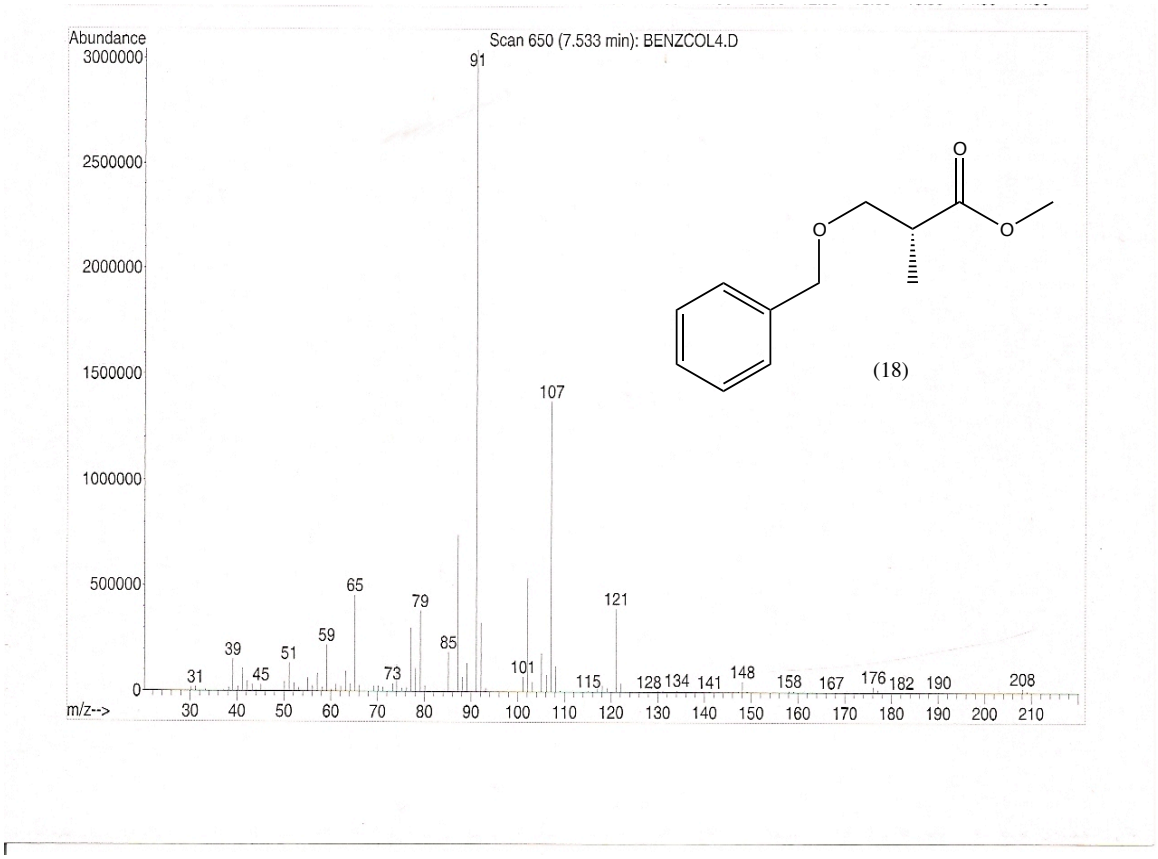

(18)

Appendix 2: ^{1}H NMR of compound 19.

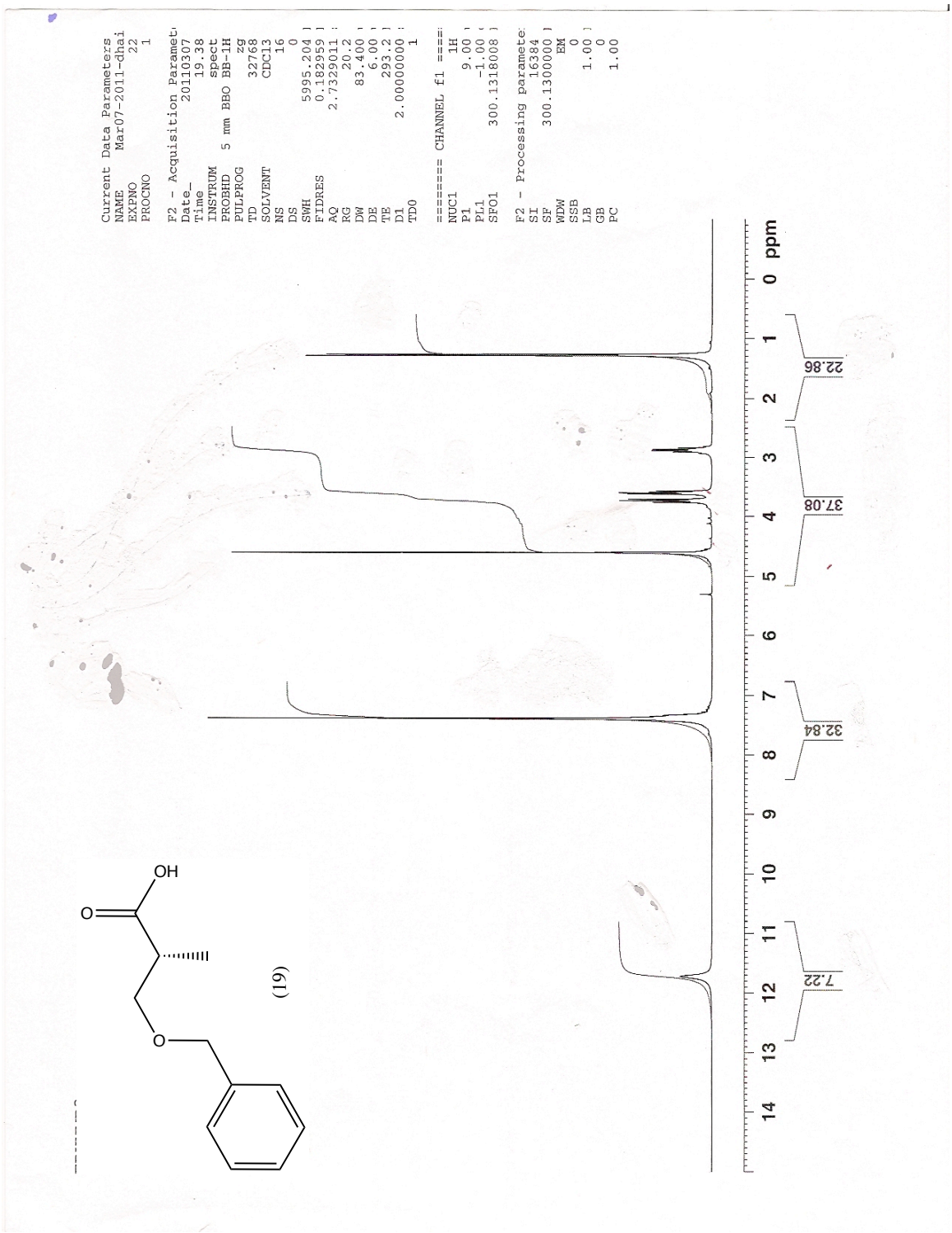

Appendix 3: ^{13}C NMR of compound 19.

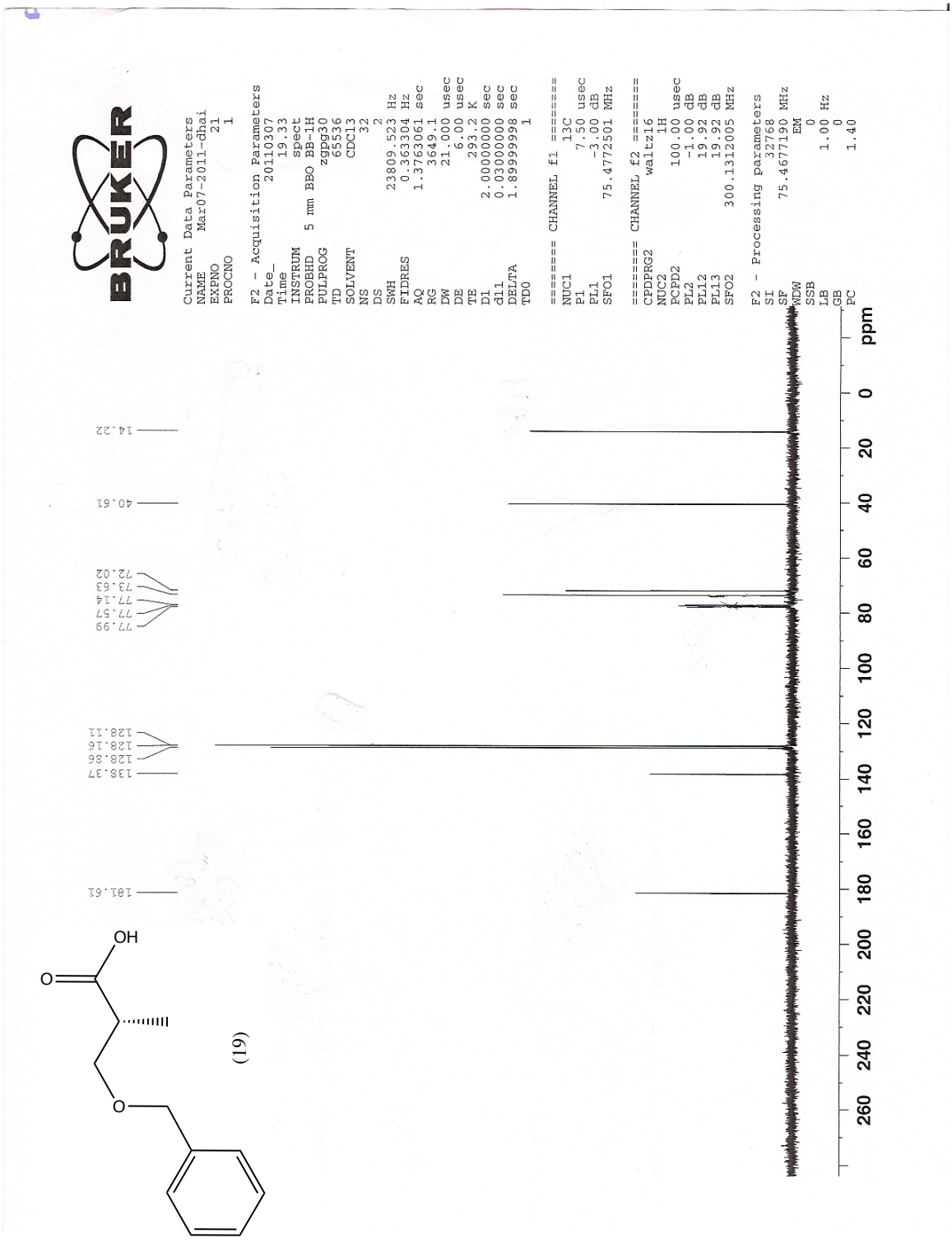

(19)

Appendix 4: ^{1}H NMR of compound 20.

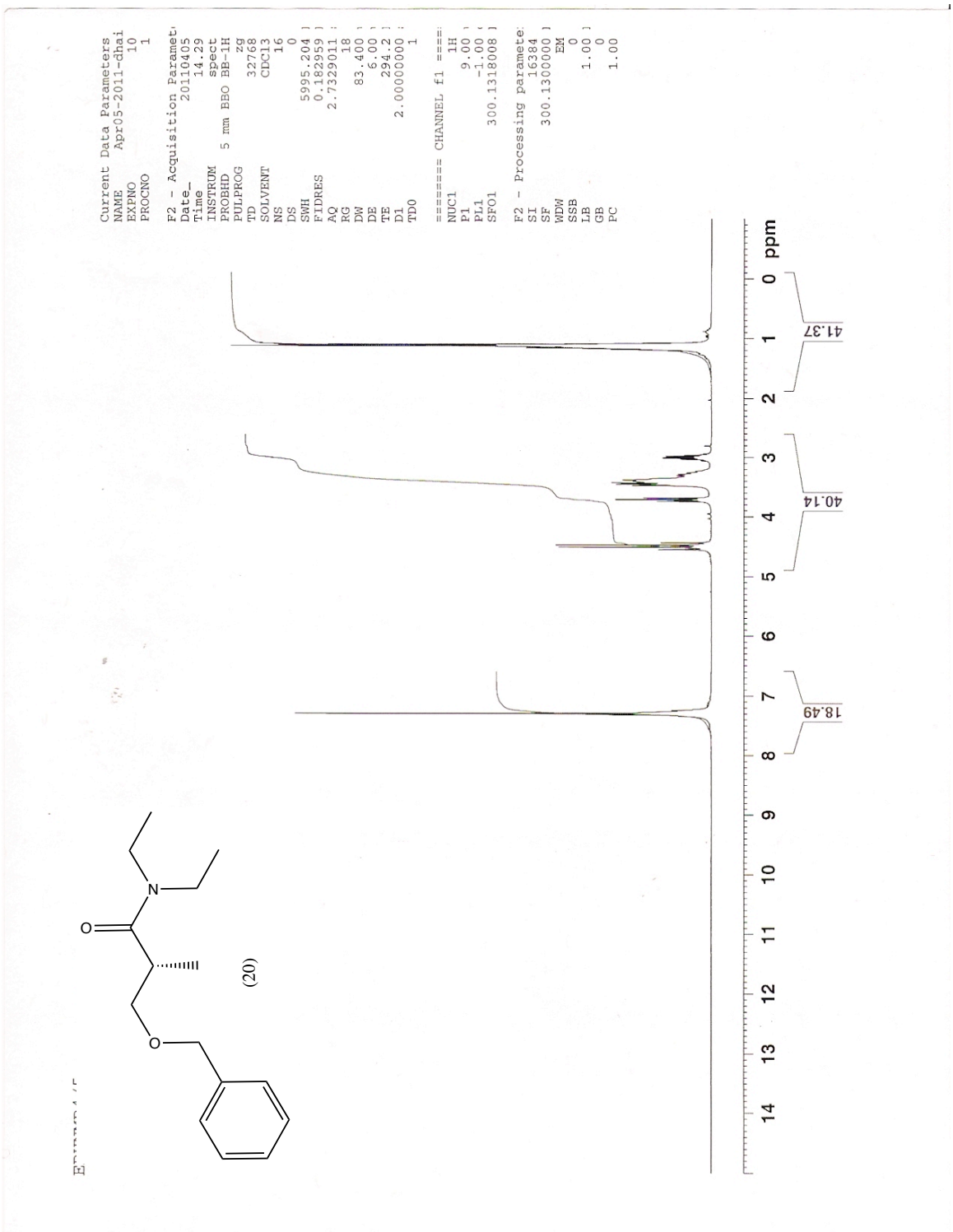

Appendix 5: ^{13}C NMR of compound 20.

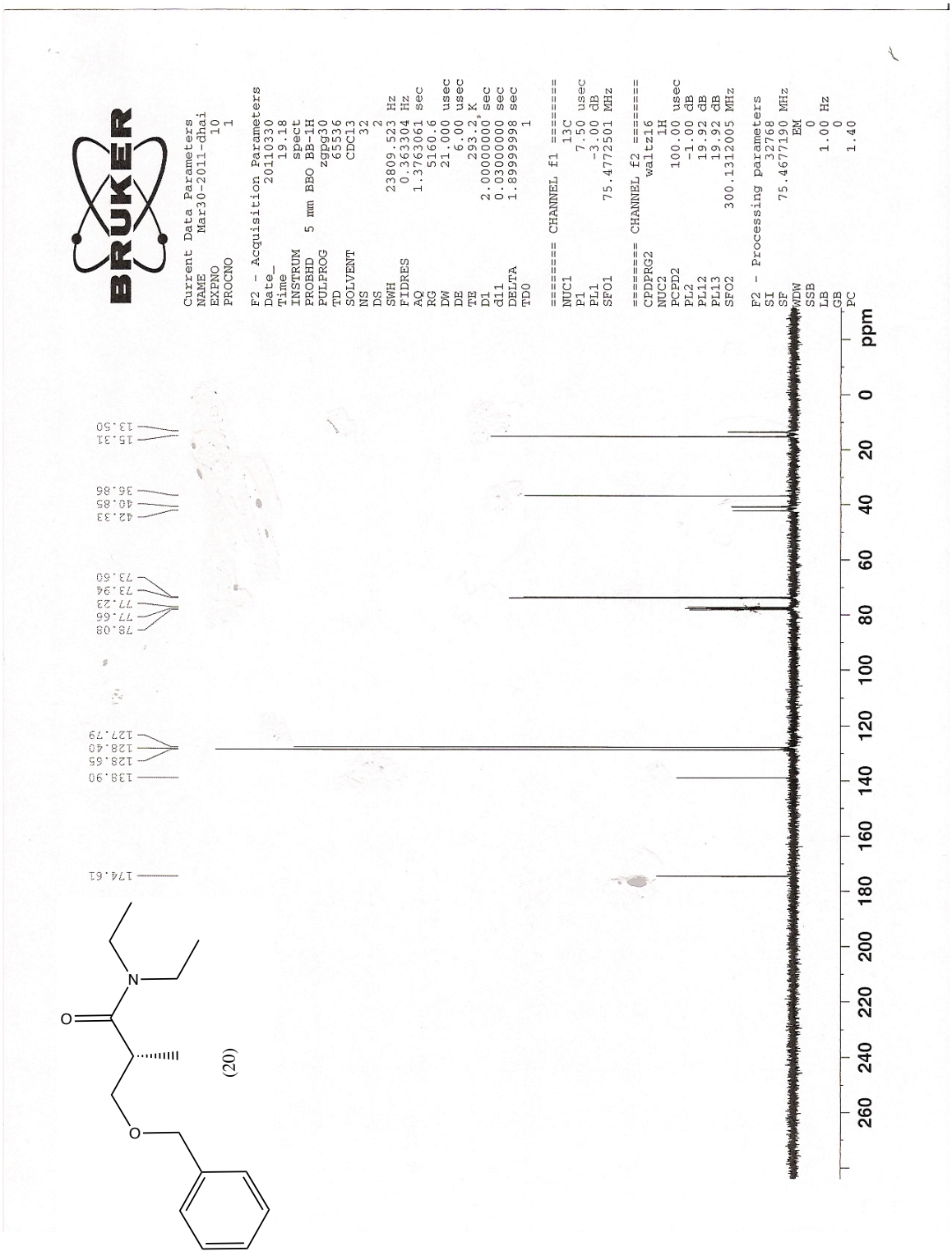

Appendix 6: ^{1}H NMR of compound 21.

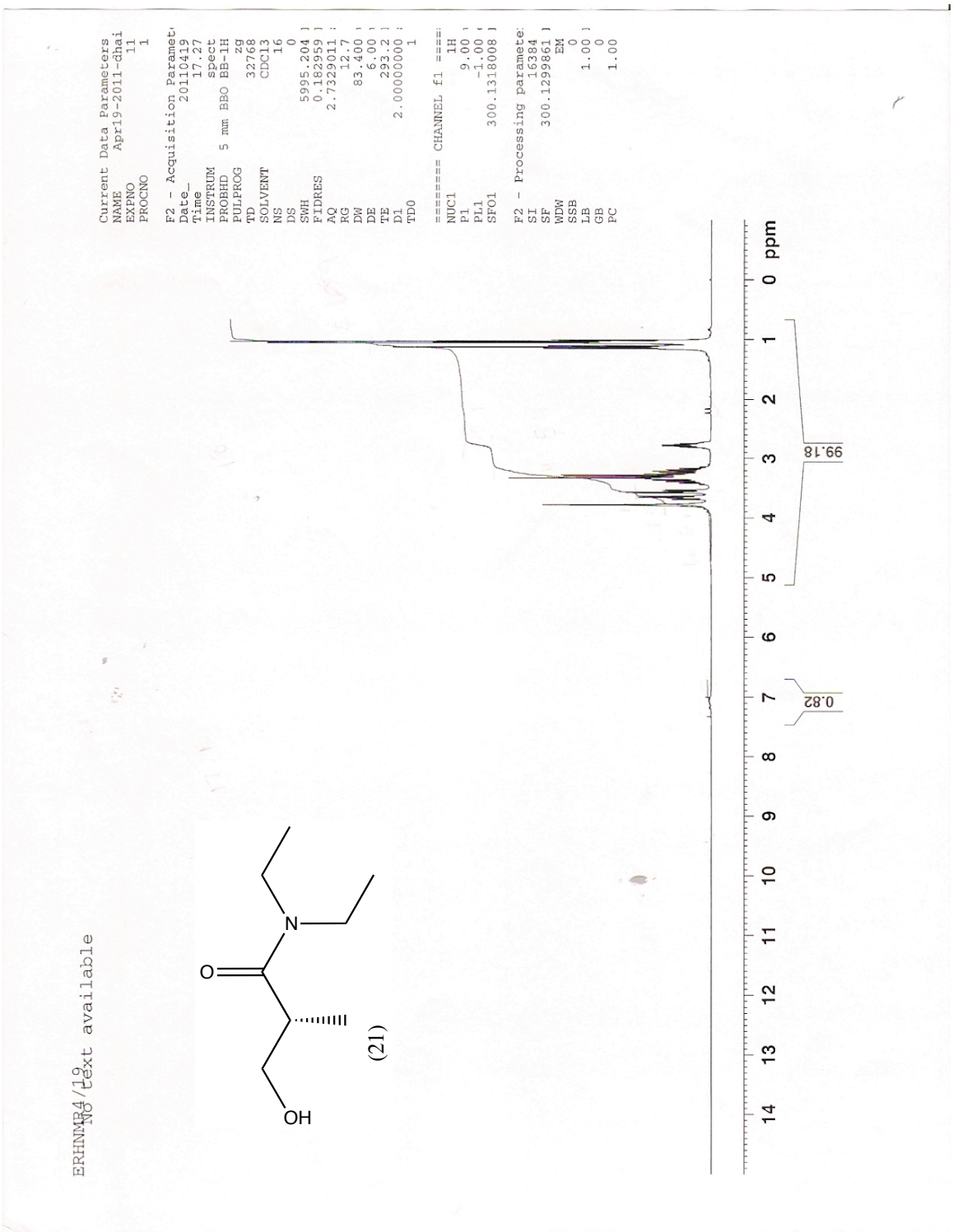

Appendix 7: ^{13}C NMR of compound 21.

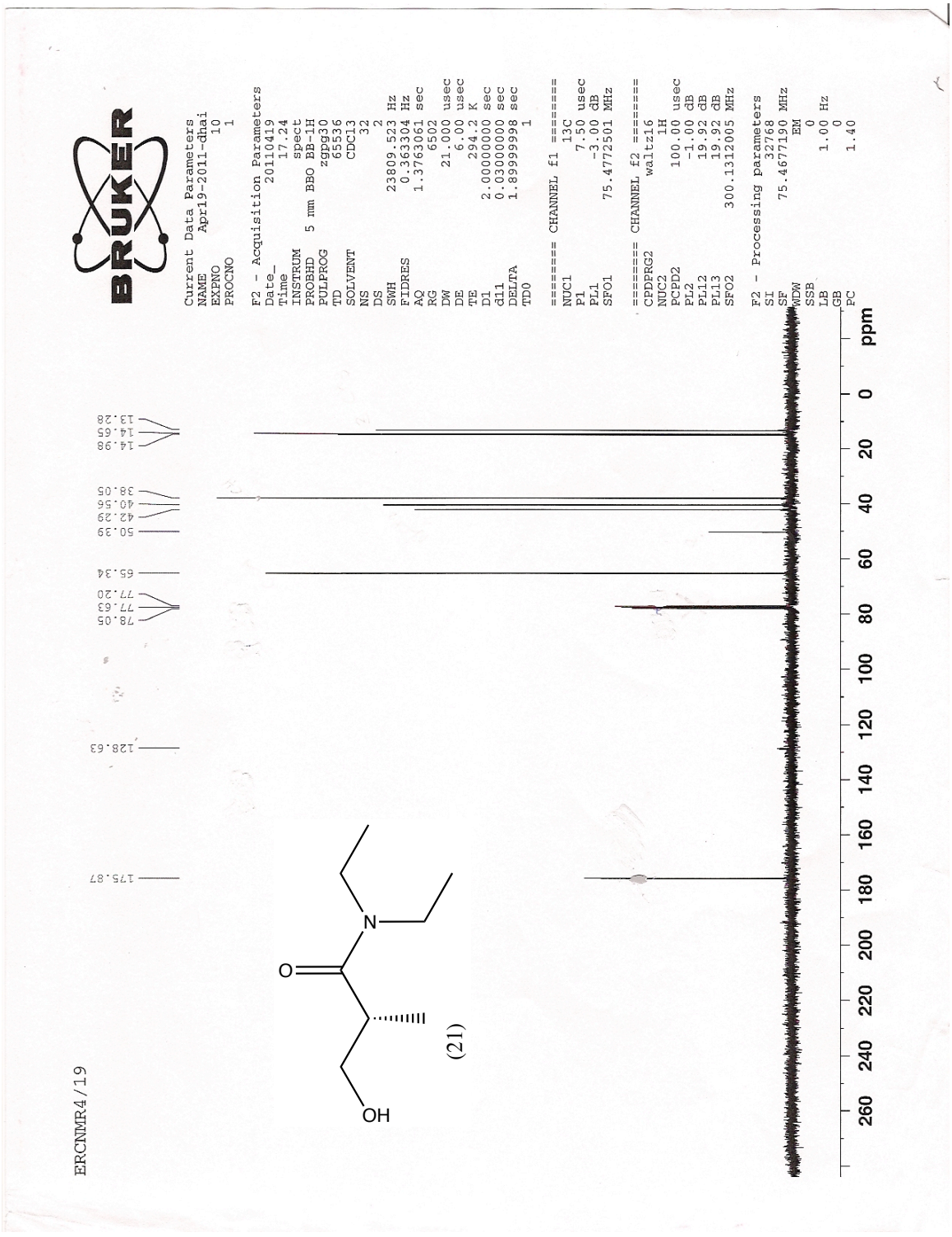

Appendix 8: ^{1}H NMR of compound 10.

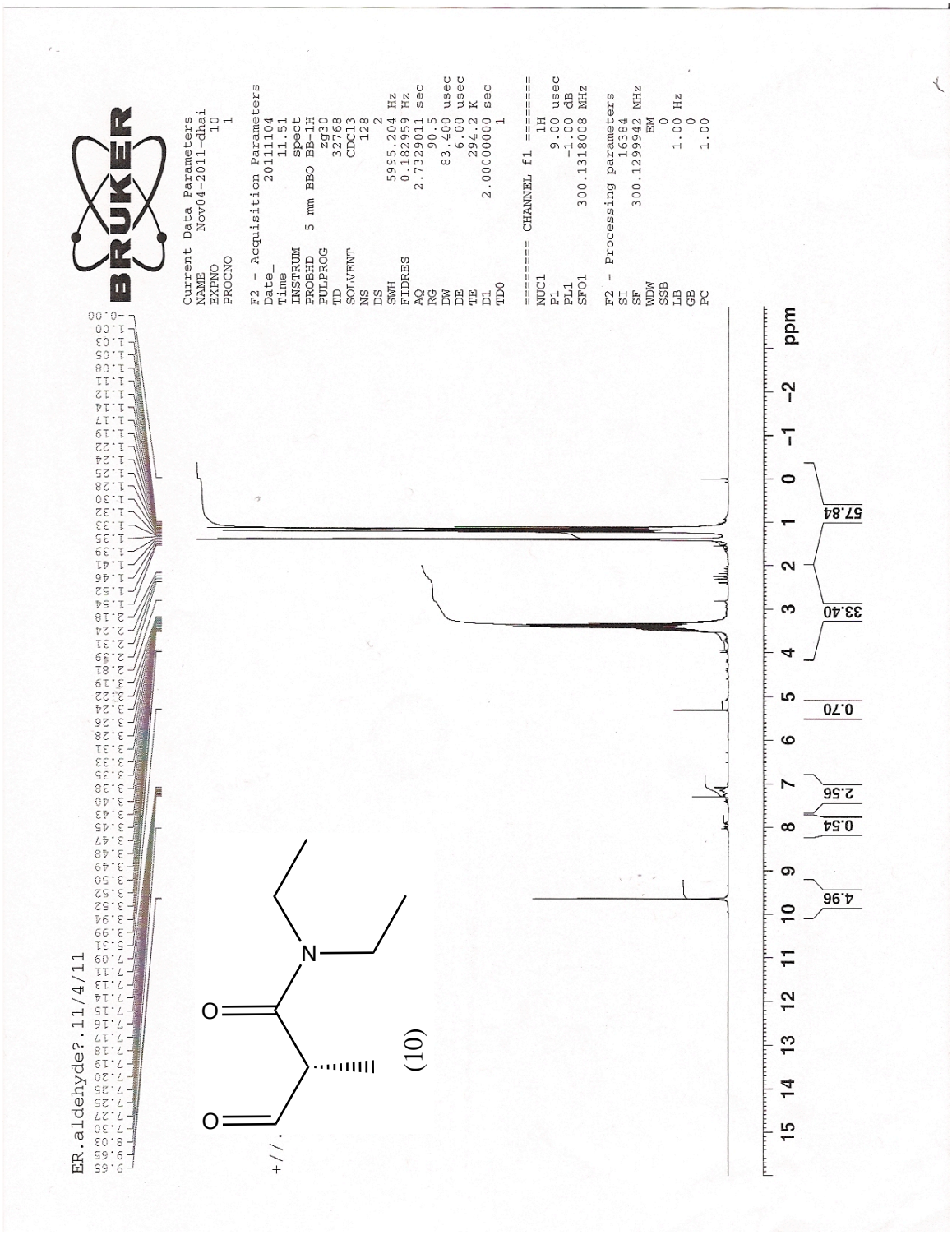

Appendix 9: ^{13}C NMR of compound 10.

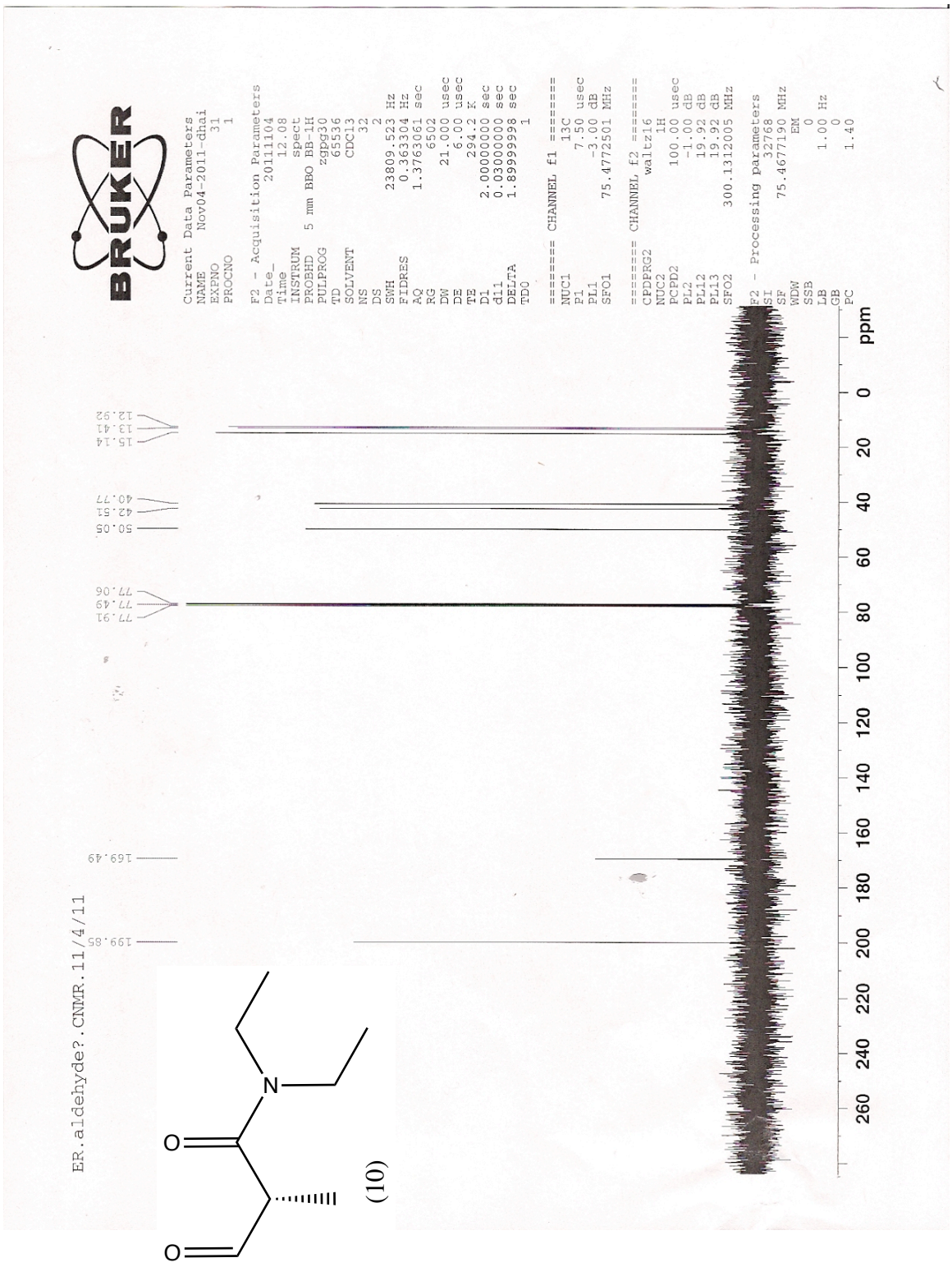

Appendix 10: ^{1}H NMR of compound 24.

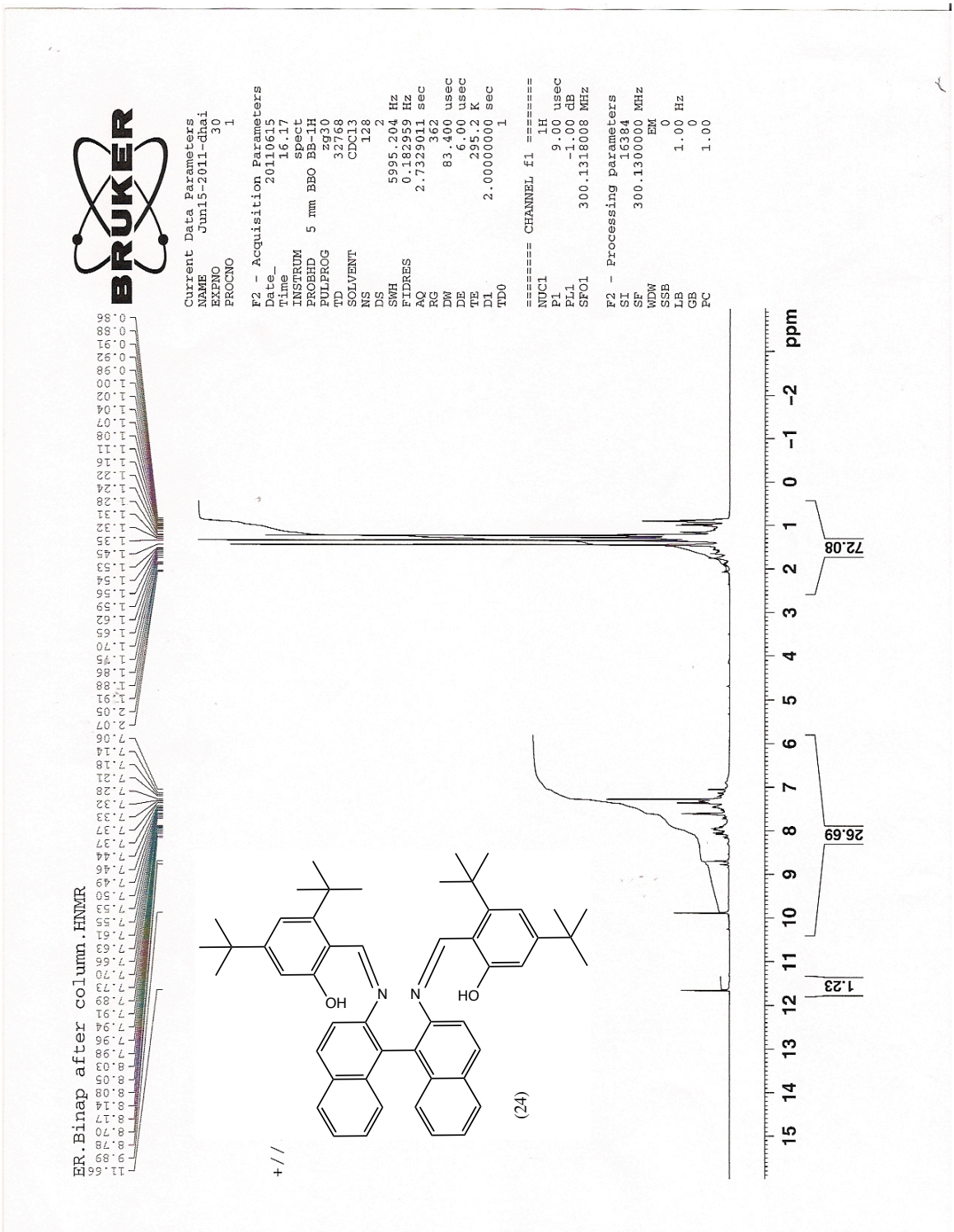

Appendix 11: ^{1}H NMR of compound 6.

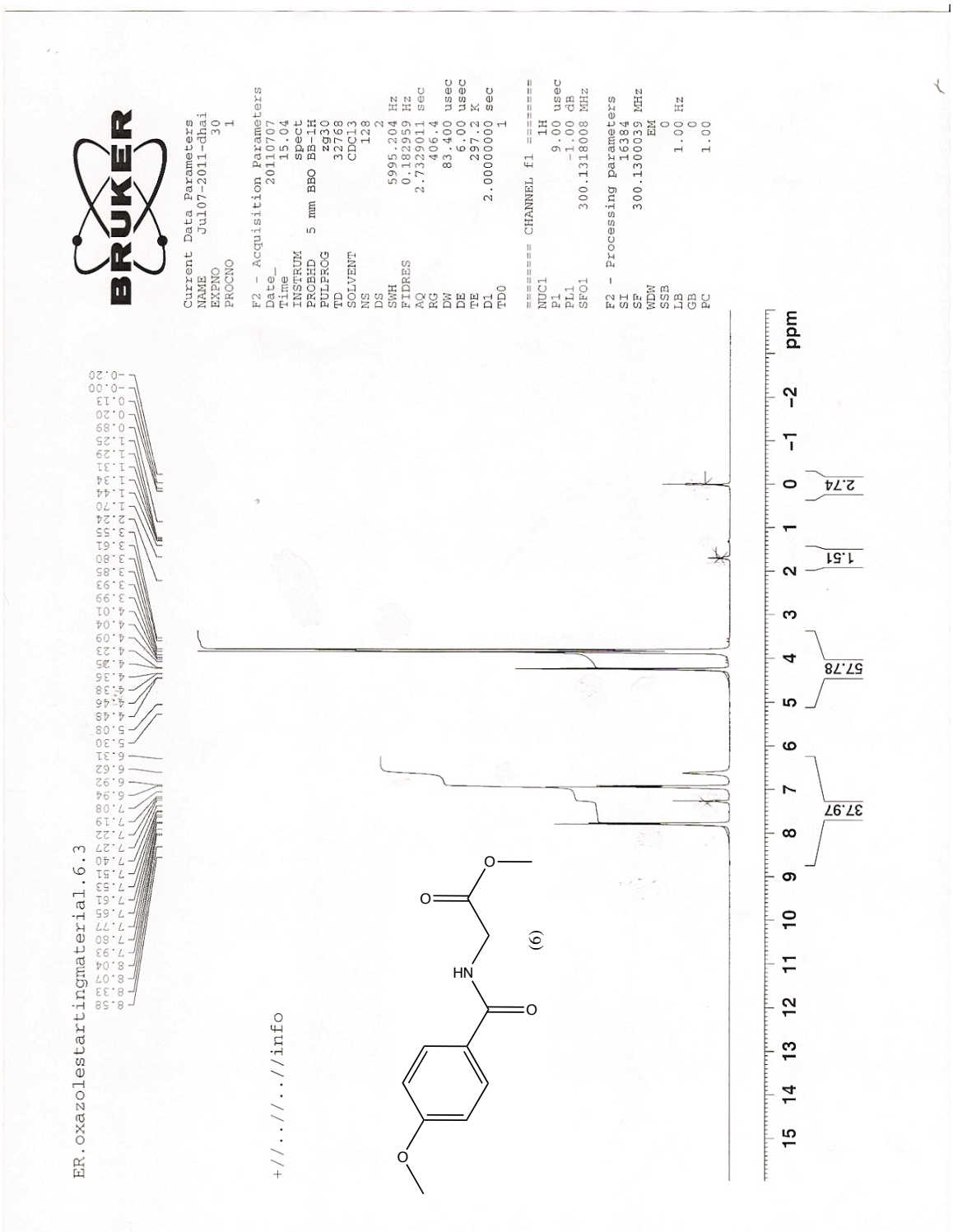

Appendix 12: ^{1}H NMR of compound 7.

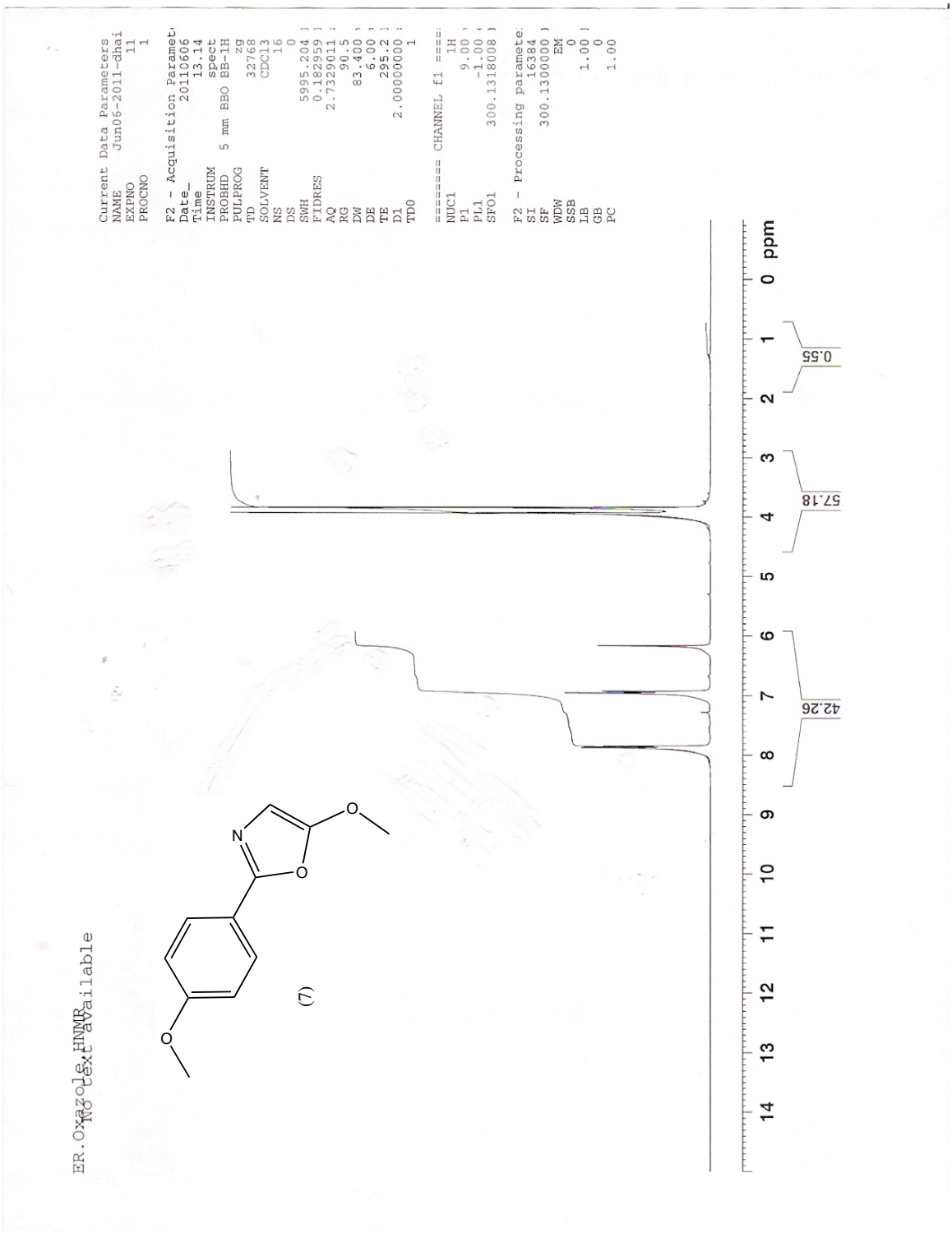

Appendix 13: ^{13}C NMR of compound 7.

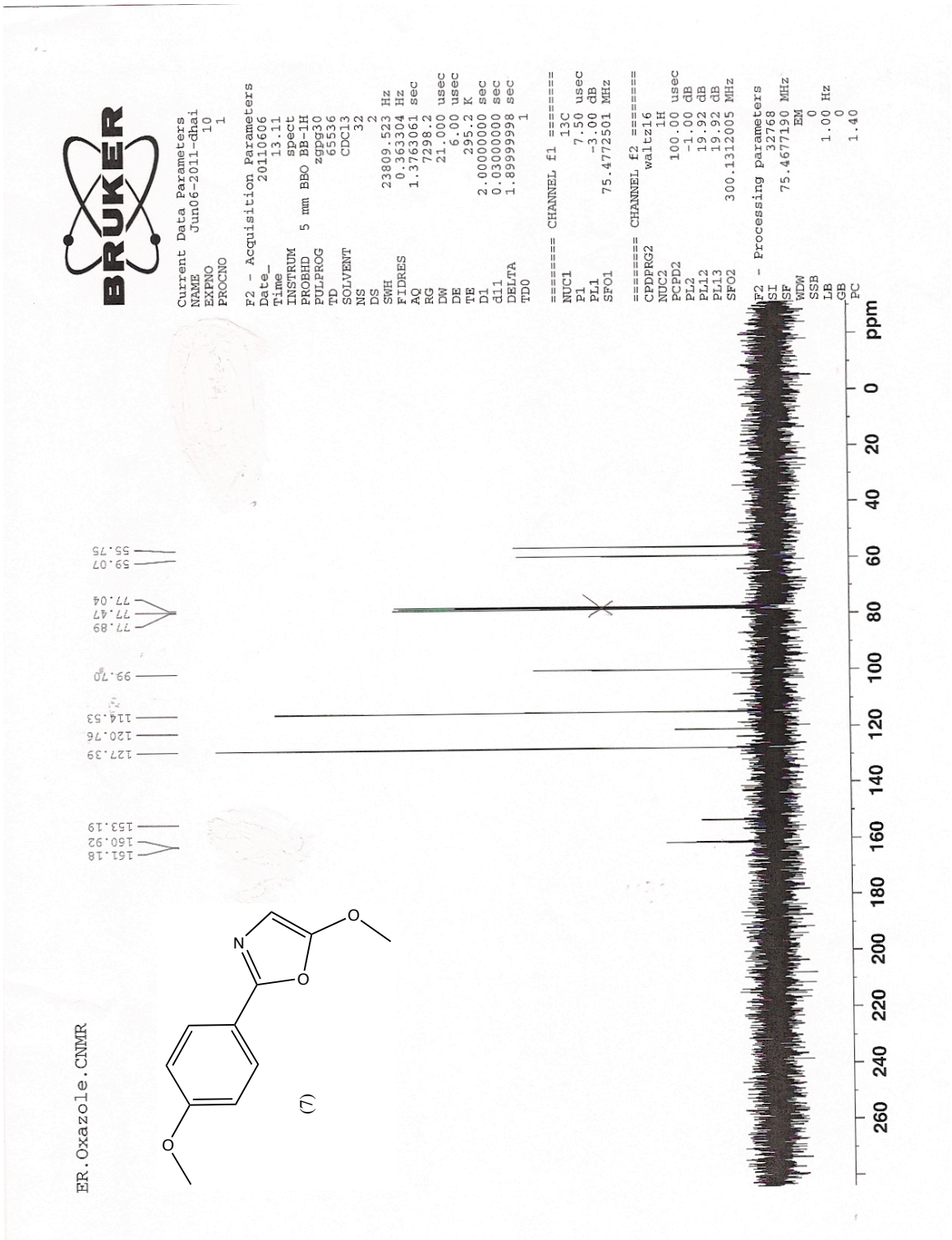

Appendix 14: ^{1}HNMR of compound 9.

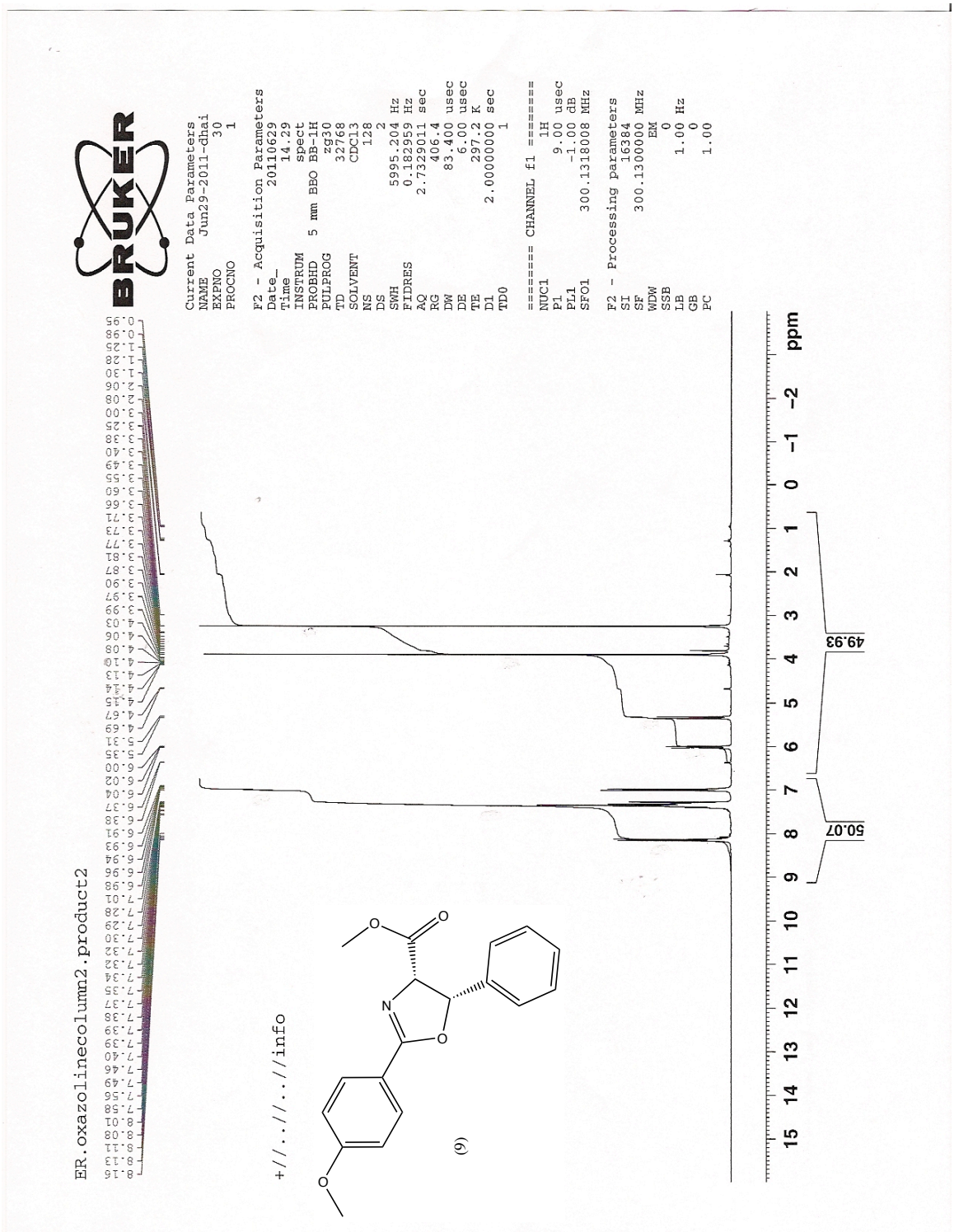

Appendix 15: ^{1}HNMR of compound 11.